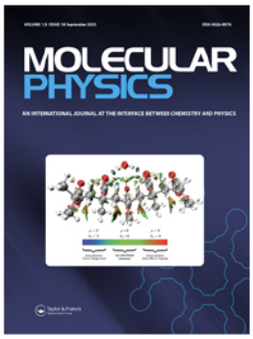

Taylor & Francis
Taylor & Francis Group

Molecular Physics

An International Journal at the Interface Between Chemistry and Physics

ISSN: 0026-8976 (Print) 1362-3028 (Online) Journal homepage: www.tandfonline.com/journals/tmph20

Estimating vertical core-excitation energies from Møller–Plesset theory with spin projection

Abdulrahman Y. Zamani & Hrant P. Hratchian

To cite this article: Abdulrahman Y. Zamani & Hrant P. Hratchian (04 Sep 2024): Estimating vertical core-excitation energies from Møller–Plesset theory with spin projection, Molecular Physics, DOI: 10.1080/00268976.2024.2398142

To link to this article: https://doi.org/10.1080/00268976.2024.2398142

MOLECULAR PHYSICS e2398142
https://doi.org/10.1080/00268976.2024.2398142

Taylor & Francis
Taylor & Francis Group

2024 SANIBEL PROCEEDINGS

Estimating vertical core-excitation energies from Møller–Plesset theory with spin projection

Abdulrahman Y. Zamani and Hrant P. Hratchian

Department of Chemistry and Biochemistry & Center for Chemical Computation and Theory, University of California, Merced, CA, USA

ABSTRACT

Spin projected ΔUHF and ΔUMP*n* ($n = 2, 2.5, 3$) methods are used to calculate vertical core excitation energies. These methods are applied to a set of symmetrical molecules with equivalent atoms. We assess the role of core localisation, SCF orbital relaxation, pair correlation, and different relativistic corrections on the accuracy and reliability of the results. Additionally, we explore the limitations of using core-hole reference determinants and address some complications that may arise in perturbative calculations.

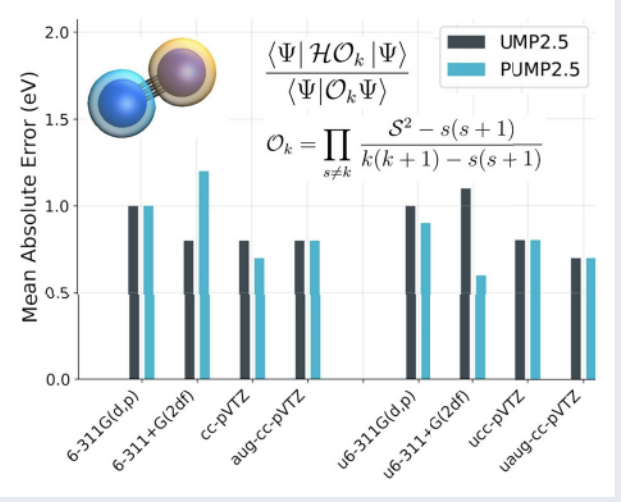

ARTICLE HISTORY
Received 2 May 2024
Accepted 20 August 2024

KEYWORDS
Vertical K-edge transitions; core-excitation; spin-projection; X-ray spectroscopy simulation

1. Introduction

High resolution X-ray spectroscopy is widely used to obtain insights into the electronic and geometric structure of condensed and gaseous matter [1–8]. Advances in experimental techniques, such as X-ray photoelectron spectroscopy (XPS), X-ray absorption spectroscopy (XAS), and inner-shell electron energy loss spectroscopy (ISEELS), have facilitated analysis of atom-specific core-level ionisations and excitations, both of which provide information relevant for 'molecular fingerprinting' and probing the photophysics of materials [9–11]. Recent endeavors for exploring ultrafast processes under X-ray radiation have revealed key information on the chemical reactivity and dynamics of many compounds, including transition metal catalysts, semiconductor thin films, battery materials, and organic molecules, by enabling observable evolution of electronic excited states [12–16]. For a particular system of interest, the unique spectroscopic signatures of an inner-shell photodetachment or excitation is dependent on the nature of the core-hole state, its sensitivity to the local environment, and the electronic structure of the final states.

Growing research in X-ray science has led to the increasing availability of high resolution experimental data. This has motivated the development of theoretical and computational approaches for simulating X-ray

CONTACT Hrant P. Hratchian hhratchian@ucmerced.edu Department of Chemistry and Biochemistry & Center for Chemical Computation and Theory, University of California, Merced, CA 95343, USA

Supplemental data for this article can be accessed online at https://doi.org/10.1080/00268976.2024.2398142.

spectroscopy [17]. Thus, in corroboration with experiment, the identification of chemical shifts and potential mechanisms for ultra-fast reactivity drives the need for accurate and predictive models. Assessing the accuracy of *ab initio* methods for modelling X-ray spectroscopy requires the consideration of modern-day experimental precision in spectral measurements. For example, the use of X-ray beams of high coherence and brilliance can reduce uncertainties in peak fitting by improving the signal-to-noise ratio and energy resolution, which allows for more distinguishable spectral features [18–23]. As such, the overall resolution obtained in experiments such as XAS and XPS is most often 1 eV or less [7,24–27].

Detailed accounts of many successful *ab initio* methods for modelling excitations and ionisations of core electrons are present in the literature [28–36]. Early studies on core-ionisations of small molecules utilised the difference of self-consistent-field solutions (ΔSCF) obtained with the Roothaan–Hartree–Fock (HF) method [37–41]. Developed around the same time, Slater's $X\alpha$ method [42] gave reasonable results for optical transitions by X-ray absorption in molecules and solids. Slater's $X\alpha$ became the progenitor of transition potential and transition operator methods through its use of fractional orbital occupation numbers [43–53].

Methods based on Kohn-Sham density functional theory (DFT), modified extensions of time-dependent density functional theory (TD-DFT), and variations of the static-exchange (STEX) method have shown viability for accurate, low-cost computation of core spectra [54–70]. More recent examples of single determinant DFT methods include the restricted open-shell Kohn–Sham (ROKS) approach [71,72] and the direct application of ionisation potential (IP) corrected exchange correlation functionals [73–75]. State-of-the-art, systematically improvable approximations based on many-body response theories offer highly accurate intensities and energies for assignments of X-ray spectra. Under this description spans variations of the *GW* approximation [76–83], the algebraic diagrammatic construction [84–89] (ADC), delta-based coupled cluster (ΔCC) [90–93], the class of equation-of-motion coupled cluster (EOM-CC) methods [94–100], and related propagator methods [101,102]. Methods for combining ΔSCF with quasiparticle corrections for orbital eigenvalues have been tested recently [103,104]. Other wavefunction theories used to study X-ray spectroscopy include multireference configuration interaction [105–108] (MRCI), Monte Carlo configuration interaction [109] (MCCI), excited state mean field (ESMF) theory [110,111], non-orthogonal configuration interaction [112–114] (NOCI), restricted open configuration interaction with singles [115–117] (ROCIS), and multiconfigurational self-consistent field (MCSCF) methods [118–122].

For most post-SCF calculations, core-excited states are accessed by limiting the excitation space of substituted determinants or by employing the core-valence separation (CVS) approximation [84,123–125]. Weak electrostatic interactions between core and valence electrons justify the exclusion of certain types of configurations or Coulomb repulsion integrals, resulting in very minor effects on *K*-edge excitation energies for light atoms [126]. Due to the nuclear proximity of core electrons, scalar relativistic and perturbative spin-orbit treatments are typically performed [127–131]. Additionally, relativistic multicomponent methods have been applied to core-excitations [132–137].

The formation of a core-hole is accompanied by a significant reorganisation of the atomic or molecular electronic structure. In quantum chemistry, this particular effect can be characterised by orbital relaxation (ORX). It is known that ΔSCF with HF is able to capture ORX effects for core-level transitions when the core orbital is localised on one atom [138–142]. However, when molecular symmetry is present, core orbitals are delocalised over equivalent atoms as symmetry adapted linear combinations. One prototypical example is the $(1s\sigma_g)^{-1}$ or $(1s\sigma_u)^{-1}$ hole-state of N_2. The reorganisation or relaxation energy is then representative of the screening potential induced by the charge distribution of valence electrons in the presence of a vacant core [143,144]. Picturing this case as a simple two-site point charge model, the screened interaction energy of a delocalised core-hole is half of what it would be with a localised core-hole. ΔSCF calculations for ionisations in diatomics from either σ_g or σ_u produce only about half of the ORX energy [145], but when the core orbitals are strongly localised (i.e. as a 1s orbital on either atom), most of the ORX energy is recovered. It follows that the ORX energy is inversely proportional to the number of equivalent atomic sites that the core-hole orbitals are delocalised over [142]. If one chooses not to abandon orbital symmetry, correlation energy contributions describing pair interactions involving the delocalised core-holes must be incorporated.

By using many-body perturbation theory (MBPT) to construct a response function [146] that contains information about the hole state, one will find that fluctuation potential/self-energy expressions contain terms corresponding to correlation that will become competitive, energetically, with terms for relaxation when symmetry is present [138,141,145,147]. With localisation, the position

of the core-hole is inherently correlated with the coordinates of the redistributed electron charge density that contributes to the screening potential, and thus, the 'concepts of relaxation and correlation become inseparable' [148,149]. The accurate performance of ΔSCF calculations on local core-holes is a direct result of effectively mixing ORX and correlation effects [145].

We have merely stated simple, historically established ideas on the physical effects that must be incorporated in theoretical models for understanding molecular X-ray physics. Considering the advancements and applications described above, there remains an outstanding need to further develop models for core-level transitions that provide reliable results with reasonable and tolerable computational scaling. In most circumstances, the aforementioned classes of methods can achieve sub-electron-volt accuracy with respect to experiment, especially for systems with second-row *p*-block elements. More specifically, CI and CC methods indeed offer highly accurate *K*-edge results, but require iterative diagonalisation and solution of amplitude equations. For example, the size of a CI-like matrix is controlled by the combinatorial number of determinants generated from the defined active space. Practical CC and EOM-CC approximations for (core) excited states can scale between $\mathcal{O}(N^6)$–$\mathcal{O}(N^8)$ [100]. To elude the curse of dimensionality and the increasingly high time and space complexities that accompany these methods, one may turn to alternatives with low-order polynomial scaling. In particular, if only mainline core-level X-ray transitions dominated by one particle or one particle-hole pair are sought, a single determinant SCF method may be preferred, especially for large systems. At mean-field cost, one can take the approach of explicit orbital optimisation of two reference determinants to model ORX [150]. On a related note, one can adopt a variational coupled cluster *ansatz* that also scales $\mathcal{O}(N^4)$, with N basis functions, to include infinite order relaxation effects [151]. Similarly, correlation effects can be added systematically with MBPT(n) to nth order. A large portion of the electron correlation energy can be recovered with second-order perturbation theory. This usually requires an initial integral transformation to the molecular orbital basis that scales $\mathcal{O}(N^5)$, which remains quite affordable.

Following this notion, the goal of this work is test and evaluate protocols in this domain with established electronic structure frameworks [152]. In this study, we opt for a spin-conserving composition of both SCF and Møller–Plesset (MP) perturbation theory with scalar relativistic corrections. The performance of these methods on the computation vertical K-edge excitation energies is assessed.

2. Methods

Spin-projected UHF and UMPn ($n = 2, 2.5, 3$) calculations are performed with different basis sets, pseudopotentials, and relativistic corrections. A protocol for orbital index restrictions according to specified thresholds for suppressing errors due to small denominators is applied. This section is composed of self-contained explanations of the component theoretical and computational procedures employed herein.

2.1. Spin projection

For generating an initial SCF wavefunction, HF is selected as a fundamental, parameter-free starting point in order to mitigate delocalisation errors, self-interaction errors, and the task of curating density functional approximations [153–157]. The maximum overlap method [158–164] (MOM) is used to locate a non-Aufbau, unrestricted Hartree–Fock (UHF) solution representing a core-hole state. To obtain a representative excited state SCF solution, a core orbital is rotated into the virtual space in accordance with the desired transition. Each iteration is then anchored to the initial guess via a projection operator and the orbital ordering is sorted by an overlap metric [161]. This method avoids variational collapse to the ground state, although other efficient algorithms are also applicable [51,72,165,166]. The excited state singlet is ideally a linear combination of open-shell configurations since the promotion of either an up-spin α or down-spin β electron from the same core orbital to some virtual orbital is equally probable. Since the chosen model is constrained to a single determinant framework, the core-hole UHF solution will suffer from artificial spin contamination as a consequence of breaking spin-symmetry in exchange for a lower energy [167–170].

To obtain correct spin-state energetics starting from a broken-symmetry solution, one can employ projection-after-variation techniques. One such method is approximate projection (AP) [171–173]. A limitation of AP is that calculation of additional $(s+1)$ spin states (themselves susceptible to spin contamination) is required if more than one contaminant is present – highlighting an insufficiency in the two-state model. Another drawback is that AP alone does not correct the wavefunction.

Furthermore, a UHF wavefunction after a single annihilation may exhibit an anomalous increase [174] in the value of the total spin-squared expectation value $\langle \mathcal{S}^2 \rangle$ away from its true $s(s+1)$ eigenvalue or, in some circumstances, $\langle \mathcal{S}^2 \rangle$ can even become negative [175]. As such, it may become necessary to remove multiple contaminants of higher spin. Determining the weighted contributions

from higher spin states will require information about higher moments m of $\langle \mathcal{S}^2 \rangle$ – the values of $\langle \mathcal{S}^{2m} \rangle$. To initiate spin purification of the broken-symmetry UHF solution, the wavefunction must be corrected.

Projected HF (PHF) wavefunctions are constructed by re-coupling intrinsic electronic spin using projection operator [176–179] or group-theoretical [180–184] techniques. PHF wavefunctions are multiconfigurational spin eigenfunctions and include the necessary nondynamical correlation in the many-electron system. Here, we employ Löwdin's spin projection operator $\mathcal{O}_k$

$$\mathcal{O}_k = \prod_{s \neq k} \frac{\mathcal{S}^2 - s(s+1)}{k(k+1) - s(s+1)} \tag{1}$$

where k is the spin of the target spin state and s is the spin of the higher state to project out. The operator $\mathcal{O}_k$ can resolve a vector in Hilbert space into its component along the axis for k spin via orthogonal projection [185]. In addition to its commutation with the spin-free nonrelativistic Hamiltonian $\mathcal{H}$, this projector satisfies characteristic properties of idempotency and completeness. $\mathcal{O}_k$ can be written as a product of annihilation operators $\mathcal{A}_k$,

$$\mathcal{A}_k = \frac{\mathcal{S}^2 - k(k+1)}{\langle \Psi_0 | \mathcal{S}^2 | \Psi_0 \rangle - k(k+1)} \tag{2}$$

which are not idempotent [186]. Applying all possible annihilators for obtaining the entire manifold of configuration state functions (CSF) is analogous to performing full CI (FCI), so truncation becomes computationally necessary.

The many-electron total spin-squared operator [187] is then

$$\mathcal{S}^2 = -\frac{N(N-4)}{4} + \sum_{i>j} \mathcal{P}_{ij}^{\zeta} \quad \zeta = \frac{N!}{2!(N-2)!} \tag{3}$$

where ζ is the number of unique two-index spin transposition generators $\mathcal{P}_{ij}$ of the symmetric group S_N containing N particles [188]. Application of $\mathcal{O}_k$ on some reference wavefunction Ψ_0 gives a CSF Φ_k that is a linear combination of Slater determinants D_j that span the subspace of basis vectors with M_k quantum numbers

$$|\Phi_k\rangle = \sum_j c_j |D_j\rangle \tag{4}$$

such that

$$\mathcal{S}^2 |\Phi_k\rangle = k(k+1) |\Phi_k\rangle . \tag{5}$$

The configuration weights $\{c_j\}$ are sometimes referred to as the Sanibel coefficients [189]. The PHF wavefunction, its energy, and spin properties should correspond to an electronic state of a particular multiplicity. The solution of the PHF equations constitutes a variation-after-projection (VAP) approach if the projected wavefunction is itself variationally optimised prior to projection [190,191]. This kind of approach is a hallmark of the extended Hartree–Fock (EHF) method [178,192]. Projection-after-variation (PAV) assumes one optimises a UHF determinant and subsequently performs spin-projection. This is known as projected UHF or PUHF [193–195] which falls under the category of EHF schemes [196]. We take advantage of the robustness of modern SCF solvers and fast convergence of single reference SCF densities to optimise UHF wavefunctions for subsequent spin projection. Importantly, the PUHF model does not include dynamical correlation contributions.

2.2. Projected Hartree–Fock and Møller–Plesset theory

To introduce information about electron-electron correlations, we treat many-body interactions perturbatively via Møller–Plesset partitioning [197] of $\mathcal{H}$ into the zeroth-order Hamiltonian $\mathcal{H}_0$ and perturbation operator $\mathcal{V}$:

$$\mathcal{H} = \mathcal{H}_0 + \mathcal{V}. \tag{6}$$

At second order, a minimal description of pair correlation corrections to the HF energy is brought about through connected doubles substitution operators $\mathcal{X}_{ij}^{ab}$. The set of $\mathcal{X}_{ij}^{ab}$ correlators are said to have isolated effects in that there is no coupling between double substitutions. In the context of core-hole states, the second-order $\langle \mathrm{OO}||\mathrm{VV} \rangle$ terms allow for pairwise core-core, core-valence, and valence-valence Coulomb and exchange interactions.

This works parallels earlier computational studies demonstrating that ΔMP2 can be used to obtain core electron binding energies with high efficiency [198,199]. On this note, Brumboiu and Fransson have performed MP2 energy decomposition analysis for core IPs [200]. Their findings indicate very large energy contributions from core-valence corrections with delocalised symmetry orbitals (see Fig. 7 of Ref. [200]). This is significant in regards to the SCF picture of an ionisation of a delocalised core orbital because, in a sense, one is removing only 'half' the core electron density. In N_2, for example, the ORX energy of a core-ionised state formed by a detatchment of $1s\sigma_u$ must be complemented by the correlation energies that describe pair-removal and pair correlations that involve both $1s\sigma_u$ and $1s\sigma_g$ – quantities that ΔSCF lacks. This reasoning translates to core-excitations as well. Take a single orbital rotation of $1s\sigma_u$ and $2p\pi_g$. ΔSCF does not have the very large core-valence corrections involving

$1s\sigma_u^{-1}$ or the remaining occupied $1s\sigma_g$. Another interesting point in the study of Brumboiu and Fransson is the large contributions of opposite spin $\alpha\beta$ and same spin $\beta\beta$ terms in the core-valence MP2 corrections for the ionisation of a delocalised α core orbital. An earlier work by Kosugi [201] also signifies the occurrence of large core-valance exchange integrals for core-hole states in diatomics (see Table 2 of Ref. [201]). The physical basis of this observation along with the considerable β ORX discourages the use of spin-component-scaled MP methods. The spin polarisation in the final state can result in a high degree of spin contamination in the UHF reference, which is a cause for severe errors in the UMP*n* series [202]. We propose, quite simply, that PUMP2 and PUHF can be chosen to remedy spin-symmetry breaking.

Because MP2 typically overestimates the pair correlation energy, MP3 is said to offer a more realistic description of that energy [203]. It may be reasonable to suggest roughly extrapolating the perturbation series by adding some fraction of the third-order correction to the second-order total energy. Methods that rely on the arithmetic mean of second- and third-order corrections have shown promising results for modelling non-covalent interactions, [204,205] reactivity, [206] and spectroscopy [207]. Since we are concerned with excitation gaps, we desire more direct information about total energies through ΔPUHF, ΔPUMP2, and ΔPUMP3.

In this paper, we adopt the formulations for spin projection outlined by Schlegel [208]. The energy for some projected reference wavefunction Ψ is given by

$$\frac{\langle \mathcal{O}_k\Psi|\,\mathcal{H}\,|\mathcal{O}_k\Psi\rangle}{\langle \mathcal{O}_k\Psi|\mathcal{O}_k\Psi\rangle}. \tag{7}$$

Since

$$[\mathcal{H},\mathcal{O}_k]=0, \tag{8}$$

the following matrix elements are equivalent:

$$\frac{\langle\Psi|\,\mathcal{O}_k{}^\dagger\mathcal{H}\mathcal{O}_k\,|\Psi\rangle}{\langle\Psi|\,\mathcal{O}_k{}^\dagger\mathcal{O}_k\,|\Psi\rangle}=\frac{\langle \mathcal{O}_k\Psi|\,\mathcal{H}\,|\mathcal{O}_k\Psi\rangle}{\langle \mathcal{O}_k\Psi|\mathcal{O}_k\Psi\rangle}. \tag{9}$$

To formulate projected energy expressions, Löwdin suggested that expectation values be evaluated for a composite Hamiltonian [178,196]

$$\mathbf{\Omega}=\mathcal{O}_k{}^\dagger\mathcal{H}\mathcal{O}_k \tag{10}$$

which can be reduced to

$$\mathcal{O}_k{}^\dagger\mathcal{H}\mathcal{O}_k=\mathcal{H}\mathcal{O}_k \tag{11}$$

because

$$\mathcal{O}_k=\mathcal{O}_k{}^\dagger\mathcal{O}_k\quad \mathcal{O}_k{}^\dagger=\mathcal{O}_k. \tag{12}$$

The projected energy is then

$$\frac{\langle \mathcal{O}_k\Psi|\,\mathcal{H}\,|\mathcal{O}_k\Psi\rangle}{\langle \mathcal{O}_k\Psi|\mathcal{O}_k\Psi\rangle}=\frac{\langle\Psi|\,\mathcal{H}\mathcal{O}_k\,|\Psi\rangle}{\langle\Psi|\mathcal{O}_k\Psi\rangle}. \tag{13}$$

The PUHF energy expression using a zeroth-order wavefunction Ψ_0 is

$$E_{\mathrm{PUHF}}=\frac{\langle\Psi_0|\,\mathcal{H}\mathcal{O}_k\,|\Psi_0\rangle}{\langle\Psi_0|\mathcal{O}_k\Psi_0\rangle}. \tag{14}$$

To incorporate systematic, order-by-order correlation effects, a projection operator [209] that spans the subspace of substituted determinants ψ_q is inserted in Equation (14)

$$\mathcal{Q}=\sum_q |\psi_q\rangle\langle\psi_q| \tag{15}$$

This secondary orthogonal space couples to the primary model space represented by a HF wavefunction. This provides CI-like matrix elements in the perturbative expansion pertinent to *n*th order wavefunction and energy corrections.

Using $\mathcal{Q}$, we resolve the identity:

$$E_{\mathrm{PUHF}}=\sum_q\frac{\langle\Psi_0|\,\mathcal{H}|\psi_q\rangle\langle\psi_q|\mathcal{O}_k\,|\Psi_0\rangle}{\langle\Psi_0|\mathcal{O}_k\Psi_0\rangle}. \tag{16}$$

By Brillouin's theorem, $\langle\Psi_0|\,\mathcal{H}\,|\psi_i^a\rangle=0$ and since $\mathcal{H}$ contains at most two-electron operators, only $\langle\Psi_0|\,\mathcal{H}\,|\psi_{ij}^{ab}\rangle$ elements are needed. Expanding Equation (16) gives

$$E_{\mathrm{PUHF}}=\langle\Psi_0|\,\mathcal{H}_0\,|\Psi_0\rangle+\sum_{\substack{i<j\\a<b}}\frac{\langle\Psi_0|\,\mathcal{V}|\psi_{ij}^{ab}\rangle\langle\psi_{ij}^{ab}|\mathcal{O}_k\,|\Psi_0\rangle}{\langle\Psi_0|\mathcal{O}_k\Psi_0\rangle}. \tag{17}$$

Determination of E_{PUHF} is straightforward since Ψ_0 can be readily computed a with a known set of single-particle basis functions. The projected wavefunction with the $\mathcal{Q}$ basis is:

$$\mathcal{O}_k\,|\Psi_0\rangle=|\Psi_0\rangle+\sum_q\frac{|\psi_q\rangle\langle\psi_q|\mathcal{O}_k\,|\Psi_0\rangle}{\langle\Psi_0|\mathcal{O}_k\Psi_0\rangle} \tag{18}$$

$$=|\Psi_0\rangle+|\tilde{\Psi}_0\rangle\,. \tag{19}$$

The correction to the UHF wavefunction from spin projection is then

$$\tilde{\Psi}_0=\sum_{\substack{i<j\\a<b}}\frac{|\psi_{ij}^{ab}\rangle\langle\psi_{ij}^{ab}|\mathcal{O}_k\,|\Psi_0\rangle}{\langle\Psi_0|\mathcal{O}_k\Psi_0\rangle}. \tag{20}$$

However, for the nth order projected energy, the wavefunction corrections up to Ψ_{n-1} will involve substitutions beyond singles ψ_i^a and doubles ψ_{ij}^{ab} due to the evaluation of $\langle \mathcal{S}^2 \rangle$ by modified Slater-Condon rules [210,211].

The projected UMPn energy is

$$E_{\mathrm{PUMP}n} = \frac{\langle \Psi_0 | \, \mathcal{H}\mathcal{O}_k \, | \Psi_0 + \Psi_1 + \ldots + \Psi_{n-1} \rangle}{\langle \Psi_0 | \, \mathcal{O}_k \, | \Psi_0 + \Psi_1 + \ldots + \Psi_{n-1} \rangle}. \quad (21)$$

Since $\mathcal{O}_k$ and $\mathcal{H}$ to commute, we get

$$E_{\mathrm{PUMP}n} = \langle \Psi_0 | \, \mathcal{H}_0 \, | \Psi_0 \rangle + \sum_q \frac{\langle \Psi_0 | \, \mathcal{V} | \psi_q \rangle \, \langle \psi_q | \mathcal{O}_k \, | \Psi_0 + \Psi_1 + \ldots + \Psi_{n-1} \rangle}{\langle \Psi_0 | \, \mathcal{O}_k \, | \Psi_0 + \Psi_1 + \ldots + \Psi_{n-1} \rangle}. \quad (22)$$

Similarly, we have expressions for E_{PUMP2} and E_{PUMP3}:

$$E_{\mathrm{PUMP2}} = \Bigg(\langle \Psi_0 | \, \mathcal{O}_k \, | \Psi_0 \rangle \, \langle \Psi_0 | \, \mathcal{H}_0 \, | \Psi_0 + \Psi_1 \rangle + \sum_q \langle \Psi_0 | \, \mathcal{O}_k | \psi_q \rangle \, \langle \psi_q | \mathcal{V} \, | \Psi_0 + \Psi_1 \rangle \Bigg) / \langle \Psi_0 | \, \mathcal{O}_k \, | \Psi_0 + \Psi_1 \rangle \quad (23)$$

$$E_{\mathrm{PUMP3}} = \Bigg(\langle \Psi_0 | \, \mathcal{O}_k \, | \Psi_0 \rangle \, \langle \Psi_0 | \, \mathcal{H}_0 \, | \Psi_0 + \Psi_1 + \Psi_2 \rangle + \sum_q \langle \Psi_0 | \, \mathcal{O}_k | \psi_q \rangle \, \langle \psi_q | \mathcal{V} \, | \Psi_0 + \Psi_1 + \Psi_2 \rangle \Bigg) / \langle \Psi_0 | \, \mathcal{O}_k \, | \Psi_0 + \Psi_1 + \Psi_2 \rangle. \quad (24)$$

Equations (23) and (24) are advantageous since one can directly control the number of $\mathcal{A}_k$ operators

Typically, spin purification is achieved after applying $\mathcal{A}_{k+1}$ and $\mathcal{A}_{k+2}$, but projection of $s > 3$ spins may still be necessary [212]. If there is only one spin contaminant, the approximation $\mathcal{O}_k \approx \mathcal{A}_{k+1}$ holds and ψ_q would contain only ψ_i^a and $\alpha\beta$ ψ_{ij}^{ab} excitations. For each $\mathcal{A}_k$, there is an instance of $\mathcal{S}^2$. Thus, m projections requires matrix elements for $\langle \mathcal{S}^{2m} \rangle$ that involve Ψ_0, ψ_{ij}^{ab}, and higher excitations in Equation (22). The less-sparse $\mathcal{S}^{2m}$ matrix for more than one annihilator reaches a spatial complexity of $\sim O^4V^4$. This approach is not very practical beyond MP2. In Equations (23) and (24), one only needs $\langle \Psi_0 | \, \mathcal{S}^2 \, | \psi_q \rangle$ where ψ_q runs over ψ_i^a and ψ_{ij}^{ab}, but at the cost of computing $\langle \psi_q | \, \mathcal{H} \, | \Psi_{n-1} \rangle$ with ψ_q going up to quadruples for PUMP2 and hextuples for PUMP3 [208].

In either forms of $E_{\mathrm{PUMP}n}$, the computation of $\mathcal{S}^{2m}$ and $\mathcal{H}$ matrix elements is similar to that of a FCI approach. Approximations to the spin projected energies can be made via Gram–Schmidt orthogonalisation of perturbative corrections Ψ_n.

$$\tilde{\Psi}_n = \Psi_n - \frac{\tilde{\Psi}_0 \langle \Psi_n | \tilde{\Psi}_0 \rangle}{\langle \tilde{\Psi}_0 | \tilde{\Psi}_0 \rangle}. \quad (25)$$

The contributions of spin projection and configurations already contained in Ψ_n are removed from the spin-projection correction of the UHF reference $\tilde{\Psi}_0$ to avoid double counting. We require, for annihilating m higher spins s,

$$\mathcal{A}_{s+m} = \frac{\mathcal{S}^2 - (s+m)(s+m+1)}{\langle \Psi_0 | \, \mathcal{S}^2 \, | \Psi_0 \rangle - (s+m)(s+m+1)} \quad (26)$$

to ensure intermediate normalisation: $\langle \Psi_0 | \mathcal{A}_{s+m} \Psi_0 \rangle = 1$ [213]. Here, we see that $\mathcal{O}_k$ is not directly applied to each Ψ_n. Rather, $\tilde{\Psi}_n$ are found using the overlaps of $\langle \Psi_n | \tilde{\Psi}_0 \rangle$.

For the limit as the set of Ψ_n and its corrections $\tilde{\Psi}_n$ approaches the exact wavefunction Ψ, the projected energy is

$$\begin{aligned} E_{\mathrm{PUMP}n} &= \langle \Psi_0 | \, \mathcal{H} \, | \Psi_0 + \tilde{\Psi}_0 + \Psi_1 + \tilde{\Psi}_1 + \cdots + \Psi_{n-1} \rangle \\ &= \langle \Psi_0 | \, \mathcal{H} \, | \Psi_0 + \Psi_1 + \cdots + \Psi_{n-1} \rangle \\ &\quad + \langle \Psi_0 | \, \mathcal{H} \, | \tilde{\Psi}_0 \rangle \\ &\quad \times \left(\frac{1 - \langle \Psi_1 + \Psi_2 + \ldots + \Psi_{n-1} | \tilde{\Psi}_0 \rangle}{\langle \tilde{\Psi}_0 | \tilde{\Psi}_0 \rangle} \right) \end{aligned} \quad (27)$$

The projected energies can be written in terms of UMPn energies combined with projected wavefunction correction terms

$$\begin{aligned} E_{\mathrm{PUMP}n} &= E_{\mathrm{UMP}n} \\ &\quad + \delta E_{\mathrm{PUHF}} \\ &\quad \times \left(\frac{1 - \langle \Psi_1 + \Psi_2 + \ldots + \Psi_{n-1} | \tilde{\Psi}_0 \rangle}{\langle \tilde{\Psi}_0 | \tilde{\Psi}_0 \rangle} \right) \end{aligned} \quad (28)$$

where

$$\delta E_{\mathrm{PUHF}} = \sum_{\substack{i<j \\ a<b}} \frac{\langle \Psi_0 | \, \mathcal{V} | \psi_{ij}^{ab} \rangle \, \langle \psi_{ij}^{ab} | \mathcal{S}^2 \, | \Psi_0 \rangle}{\langle \Psi_0 | \, \mathcal{S}^2 \, | \Psi_0 \rangle - (s+m)(s+m+1)} \quad (29)$$

is obtained from Equation (17). The expressions for this estimation at second and third order are

$$\tilde{E}_{\mathrm{PUMP2}} \simeq E_{\mathrm{UMP2}} + \delta E_{\mathrm{PUHF}} \left(\frac{1 - \langle \Psi_1 | \tilde{\Psi}_0 \rangle}{\langle \tilde{\Psi}_0 | \tilde{\Psi}_0 \rangle} \right) \quad (30)$$

and

$$\tilde{E}_{\mathrm{PUMP3}} \simeq E_{\mathrm{UMP3}} + \delta E_{\mathrm{PUHF}} \left(\frac{1 - \langle \Psi_1 + \Psi_2 | \tilde{\Psi}_0 \rangle}{\langle \tilde{\Psi}_0 | \tilde{\Psi}_0 \rangle} \right) \tag{31}$$

The approximation to PUMP3, in the $\mathcal{Q}$ space of singles, doubles, and quadruples, conventionally scales as $O(M^6)$ for M basis with the additional overhead of generating $\langle \mathcal{S}^2 \rangle$ for each annihilation. Results for UMP4 also accompany those for projected third order, but with the omission of ψ_{ijk}^{abc} terms [214]. Contributions from three-body correlations would otherwise present a steep cost of $O(M^7)$. In this work, we make use of implementations based on Equations (17), (30), and (31).

2.3. Relativistic corrections

Scalar relativistic effects for C, N, O, and F atoms are included as a *post hoc* correction to ΔHF and ΔMP excitation energies. We examine two procedures. The first is based on the relativistic shift in the ionisation potential for a two-electron atom defined by Bethe and Salpeter [215].

$$E_J = \alpha^2 \left[-\frac{1}{8} Z^4 + \frac{1}{4} \langle p_1^4 \rangle - \pi Z \langle \delta^{(3)}(\mathbf{r}_1) \rangle - \pi \langle \delta^{(3)}(\mathbf{r}_{12}) \rangle \right] - E_2 \tag{32}$$

Expectation values in E_J for atomic number $Z > 2$ are available in works by Perekis, Silverman, and Scherr [216,217]. A different correction scheme for C, N, O, and F was developed by Chong and coworkers [218–220], leading to the following formula

$$C_{rel} = \mathcal{A} I_{\mathrm{nr}}^{\mathcal{B}} \tag{33}$$

where the correction C_{rel} (in eV) is found with $\mathcal{A} = 2.198 \times 10^{-7}$, $\mathcal{B} = 2.178$, and the calculated non-relativistic core IP I_{nr} (in eV). The corrections of Perekis C_{Perekis} for atomic ions isoelectronic to helium lack valence screening present in molecules. The values of C_{Perekis} are then larger than those of C_{Chong} by a factor of ~ 2. In lieu of performing ΔSCF calculations for Equation (33), we abide by this heuristic. The relativistic corrections used in this work for C, N, O, and F are 0.1, 0.2, 0.4, 0.7 eV under C_{Perekis} and 0.05, 0.1, 0.2, 0.35 eV under C_{Chong}, respectively.

2.4. Denominator control

The MP2 energy denominator with a core-hole reference $(\epsilon_i + \epsilon_j - \epsilon_a - \epsilon_b)$ may become very small. The addition of a core-hole orbital ϵ_a with a large negative eigenvalue with a lower-lying occupied valence ϵ_i may nearly cancel the addition of another valence ϵ_j with a high-lying virtual ϵ_b that possesses a large, positive eigenvalue. Similarly, a core-hole ϵ_a plus another negative, high-energy core orbital ϵ_i combined with a valence orbital ϵ_j plus a low-lying virtual ϵ_b can lead to a very small denominator. In these cases, identical atoms can lead to greater instances of coupling between core-holes and occupied cores. Also, basis sets with many polarisation functions of high angular momentum can result in high energy virtual orbitals with eigenvalues similar in magnitude but opposite in sign to the core-orbitals. These small denominators introduce numerical instabilities in the perturbation series [90,96,200]. A recent protocol by Dreuw and Fransson [221], suggests a denominator threshold of 0.1 a.u. for freezing orbital indices for correlation. We adopt this threshold τ_L and switch on a tighter (0.02 a.u.) threshhold τ_T when the frozen orbital window with τ_L still exceeds 5% of the total orbital count.

3. Results

3.1. Computational details

Vertical K-edge excitation energies ω_X for symmetry-allowed transitions are computed using ΔUHF and ΔUMPn ($n = 2, 2.5, 3$) with and without spin projection for various combinations of basis sets. Relativistic corrections for C, N, O, and F are added to the individual energy differences. The Pople and Dunning basis sets are taken from the Basis Set Exchange [222]. Multi-electron Wood-Boring (MWB2) effective core potentials (ECP) on non-target atoms sans hydrogen are used for core-localisation. The basis sets for second-row atoms are also 1s uncontracted (u) for a more optimal core orbital. Redundant functions in the core-uncontracted Dunning basis are removed.

An assortment of symmetrical molecules with equivalent atoms listed in Table 1 were taken from the Chong-Gritsenko-Baerends (CGB) dataset [247] and the NIST CCCBDB [248]. Optimised geometries with CCSD(T)/aug-cc-pVTZ are reported in a prior publication [249] and in the CCCBDB. The structure for OF_2 was optimised locally at the same level of theory. All molecules in the test set are closed shell except O_2.

All calculations were performed with a development version of Gaussian [250]. For calculations without ECPs, integral symmetry with Abelian groups is used.

Table 1. Set of symmetrical molecules and experimental core-excitation energies at the C, N, O, and F K-edge.

C K-Edge	Exp.	N K-Edge	Exp.	O K-Edge	Exp.	F K-Edge	Exp.
C_2H_2	285.9 [223]	N_2	400.9 [224]	O_3 (**O** = O–O)	529.1 [225]	F_2	682.2 [226]
C_2H_4	284.7 [223]	*cis*-Diazene	398.4 [227]	H_2O_2	533.0 [228]	C_2F_4	690.7 [229]
C_2H_6	286.9 [223]	C_2N_2	398.9 [230]	CO_2	535.4 [231]	CF_2O	689.2 [232]
C_2N_2	286.3 [230]	Hydrazine	401.5 [233]	O_2	530.8 [234]	CH_2CF_2	690.3 [229]
Cyclopropane	287.7 [235]	Urea	402.0 [236]			*cis*-CH_2CF_2	689.3 [229]
C_2F_4	290.1 [229]	N_3^- (**N** = N = N)	399.6 [227]			OF_2	683.8 [237]
Furan (**C**–O)	286.6 [238]	Tetrazine	398.8 [239,240]			NF_3	687.4 [241]
Allene (**C** = C = C)	285.4 [242]						
Cyclobutane	287.4 [235]						
C_2	285.9 [223,243]						
Acetone (**C**–C = O)	288.4 [244]						
Pyridine (**C**–N)	285.3 [240]						
Tetrazine	285.2 [239]						
Benzene	285.2 [245]						
Pyrrole (**C**–NH)	286.3 [246]						

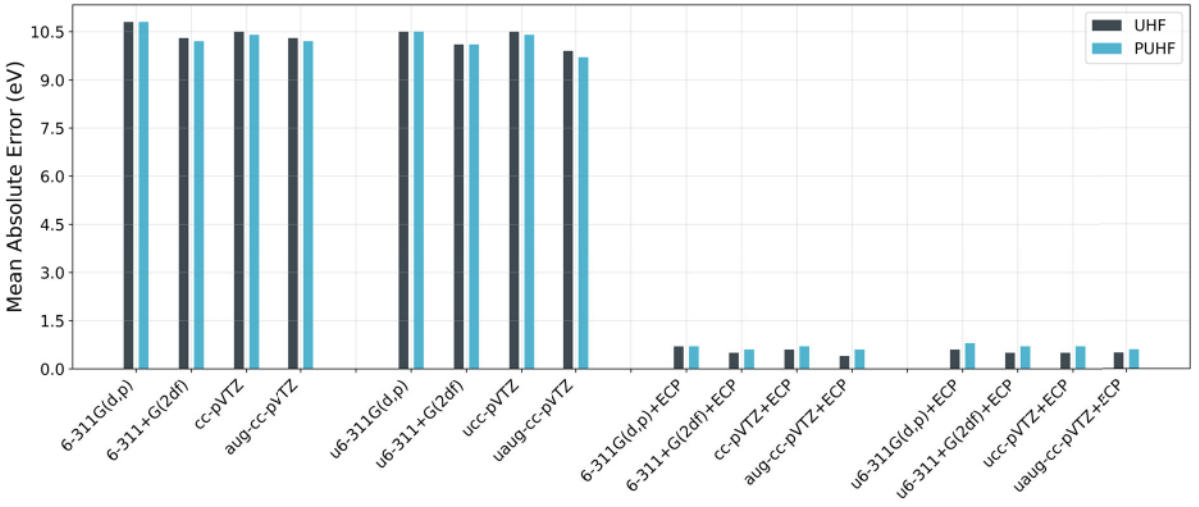

Figure 1. Mean absolute errors (eV) of UHF and PUHF for various basis set combinations.[a]

[a]Results obtained with tight threshold τ_T, relativistic correction B (C_{Chong}), and with outlier cases removed.

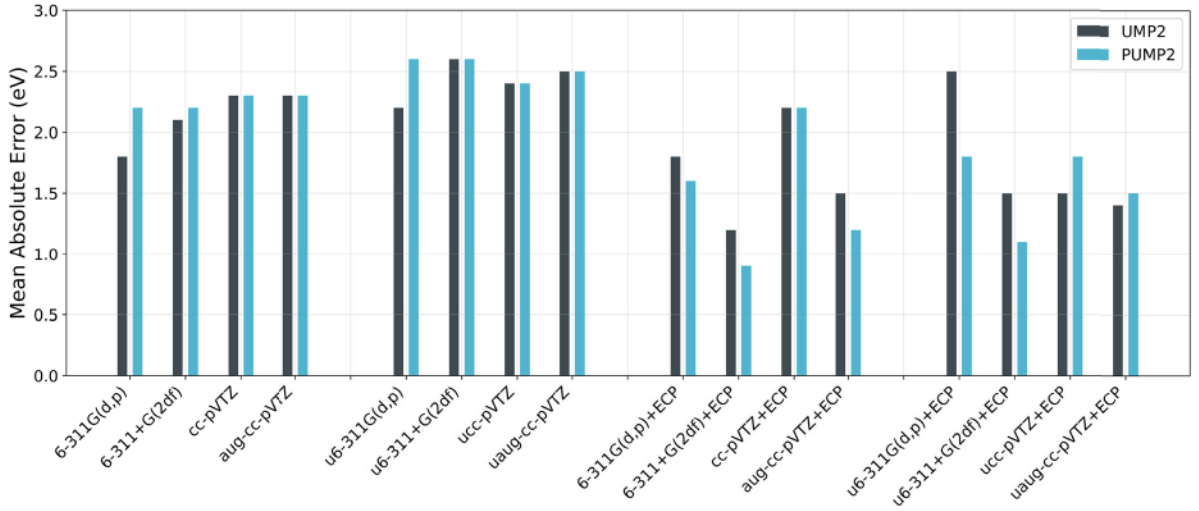

Figure 2. Mean absolute errors (eV) of UMP2 and PUMP2 for various basis set combinations.[a]

[a]Results obtained with tight threshold τ_T, relativistic correction B (C_{Chong}), and with outlier cases removed.

3.2. ΔPUHF and ΔPUMPn

The mean absolute error (MAE) and root-mean-square error (RMSE) between calculated ω_X values and experimental values are reported. Histograms with the MAE for ΔPUHF and ΔPUMPn using $\mathcal{C}_{\text{Chong}}$ are provided in this section as Figures 1–4. Detailed information about the overall data, $\langle \mathcal{S}^2_{\text{UHF}} \rangle$ and the measure of errors are available in the Supplementary Material. Spin contamination is removed from core-excited states after annihilation of spin states up to $s+3$ or $s+4$.

The performance of ΔUHF and ΔPUHF is shown in Figure 1. In all standard ΔSCF methods, there is a stark difference of ∼10 eV in the MAE between basis sets with and without core localisation by ECP. The results for ΔPUHF are similar to ΔUHF without ECPs across the standard contracted basis sets. A notable decrease in MAE occurs when going from (u)6-311G(d) to (u)6-311+G(2df) and from (u)cc-pVTZ to (u)aug-cc-pVTZ – owing to the increased variational flexibility in the SCF solutions. Localised core ΔUHF and ΔPUHF calculations offer a MAE ∼0.5–1.0 eV and RMSE ∼1 eV. No significant differences between results with contracted or uncontracted basis sets are observed for this data set. We observe that ΔPUHF+ECP energies are equal to or slightly higher than ΔUHF+ECP. This may be due to the non-variational nature of the correction to the excited state E_{UHF}, the quality of the SCF+ECP solution, or the annihilation of a lower energy triplet configuration from the open-shell singlet wavefunction – a consequence of the symmetry dilemma [167].

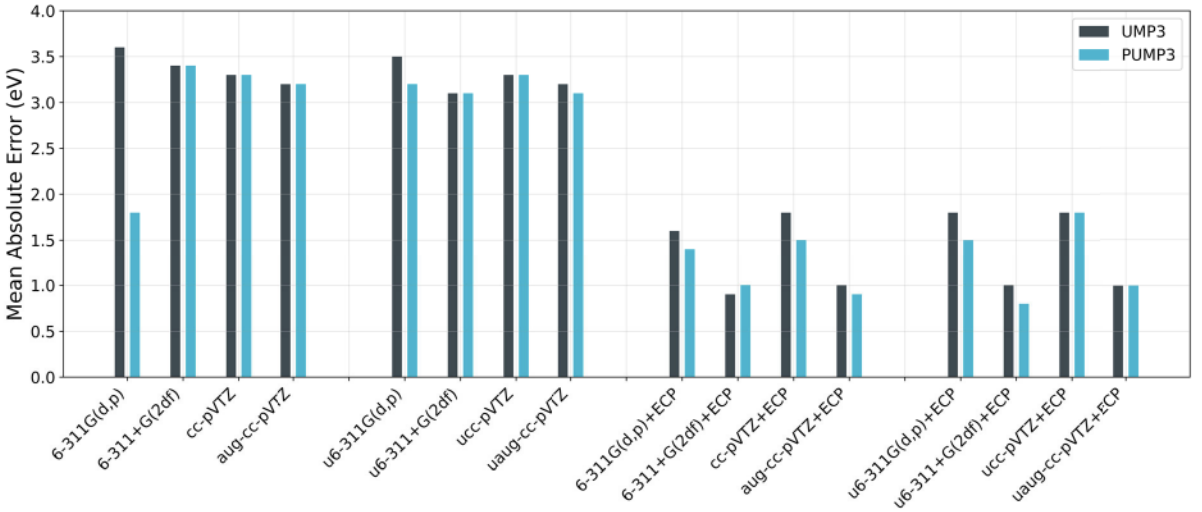

Figure 3. Mean absolute errors (eV) of UMP3 and PUMP3 for various basis set combinations.[a]

[a]Results obtained with tight threshold τ_T, relativistic correction B ($\mathcal{C}_{\text{Chong}}$), and with outlier cases removed.

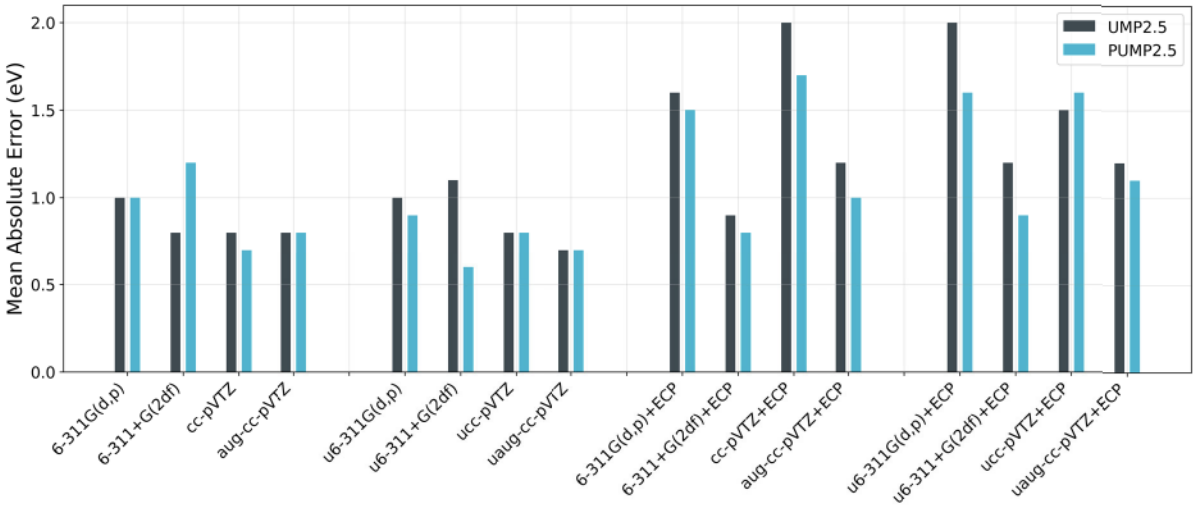

Figure 4. Mean absolute errors (eV) of UMP2.5 and PUMP2.5 for various basis set combinations.[a]

[a]Results obtained with tight threshold τ_T, relativistic correction B ($\mathcal{C}_{\text{Chong}}$), and with outlier cases removed.

In Figure 2, we show results for ΔUMP2 and ΔPUMP2. We find that second-order energies underestimate experiment by generally ∼1–5 eV (see Supplementary Material). This is expected, as the two-body corrections in MP2 typically exaggerate the correlation effects. The absolute errors for ΔUMP2+ECP and ΔPUMP2+ECP are slightly lower, more varied, and less uniform than the same results without ECPs. Signed errors in ΔUMP2+ECP and ΔPUMP2+ECP data still indicate a general overestimation with respect to experiment. Uncontracting the 1s basis function in this dataset appears to slightly increase the absolute deviation from experiment, except for (u)cc-pvtz+ECP where it decreases considerably.

Figure 3 shows results for ΔUMP3 and ΔPUMP3. The third order ω_X values generally overestimate experiment. For calculations on delocalised cores, the MAE and RMSE can reach up to ∼4 eV and ∼5 eV respectively. The MAE for ΔPUMP3/6-311G(d) that is about two times smaller than the others in its class appears coincidental since the results for other 6-311G(d) varients are generally within 1 eV of larger basis set combinations. The errors for ΔUMP3+ECP and ΔPUMP3+ECP are generally equal to or lower than their second-order counterparts. The behaviour of uncontracted versus contracted results in this dataset is inconsistent: slightly higher in some cases and slightly lower in others. The energies of both the second- and third-order methods coupled with ECPs are essentially lower than those without across all considered basis sets.

The results for ΔUMP2.5 and ΔPUMP2.5 are featured in Figure 4. For the retention of molecular symmetry, the inclusion of 50% third-order corrections ameliorates some of the deficiencies of MP2 and MP3 energies by providing ω_X values approximately halfway between. Cancellation of errors becomes less

Table 2. Measure of errors w.r.t. experiment for symmetry-allowed vertical K-edge excitation energies (eV) computed without spin projection using different combinations of the 6-311 + G(2df) basis set.[a,b].

	$\langle\overline{\mathcal{S}}^2_{\mathrm{UHF}}\rangle_{S=0}$[c]	UHF	UMP2	UMP3	UMP2.5
6-311 + G(2df)[d]	1.043				
τ_T-A-MAE		10.4 (10.4)	2.0 (2.0)	3.7 (3.5)	1.0 (1.0)
τ_L-A-MAE		10.4 (10.5)	1.9 (1.8)	4.2 (4.0)	1.6 (1.4)
τ_T-A-RMSE		10.8 (10.8)	2.3 (2.3)	4.1 (4.0)	1.4 (1.3)
τ_L-A-RMSE		10.8 (10.9)	2.3 (2.1)	4.8 (4.6)	2.3 (2.0)
τ_T-B-MAE		10.3 (10.3)	2.1 (2.1)	3.5 (3.4)	0.9 (0.8)
τ_L-B-MAE		10.3 (10.3)	2.0 (1.9)	4.1 (3.8)	1.5 (1.2)
τ_T-B-RMSE		10.6 (10.6)	2.4 (2.5)	4.0 (3.8)	1.2 (1.2)
τ_L-B-RMSE		10.6 (10.7)	2.4 (2.2)	4.7 (4.5)	2.2 (1.9)
6-311 + G(2df) & ECP[d]	1.139				
τ_T-A-MAE		0.7 (0.6)	1.0 (1.0)	0.9 (0.8)	0.8 (0.8)
τ_L-A-MAE		0.6 (0.5)	1.4 (1.3)	0.9 (0.9)	1.1 (1.0)
τ_T-A-RMSE		0.8 (0.7)	1.3 (1.2)	1.0 (1.0)	1.0 (1.0)
τ_L-A-RMSE		0.8 (0.6)	1.7 (1.6)	1.1 (1.1)	1.4 (1.3)
τ_T-B-MAE		0.7 (0.6)	1.0 (0.9)	0.9 (0.9)	0.8 (0.8)
τ_L-B-MAE		0.6 (0.5)	1.3 (1.2)	0.9 (0.8)	1.0 (0.9)
τ_T-B-RMSE		0.9 (0.7)	1.2 (1.1)	1.0 (1.0)	1.0 (1.0)
τ_L-B-RMSE		0.7 (0.6)	1.6 (1.5)	1.1 (1.1)	1.3 (1.2)
u6-311 + G(2df)[d]	1.039				
τ_T-A-MAE		10.2 (10.2)	2.4 (2.4)	3.4 (3.2)	0.8 (0.8)
τ_L-A-MAE		10.2 (10.3)	2.2 (2.1)	4.0 (3.8)	1.4 (1.2)
τ_T-A-RMSE		10.6 (10.6)	2.8 (2.8)	3.8 (3.7)	1.1 (1.1)
τ_L-A-RMSE		10.6 (10.7)	2.6 (2.4)	4.6 (4.4)	2.2 (1.9)
τ_T-B-MAE		10.1 (10.1)	2.6 (2.6)	3.2 (3.1)	0.8 (0.7)
τ_L-B-MAE		10.1 (10.2)	2.3 (2.2)	3.8 (3.6)	1.3 (1.2)
τ_T-B-RMSE		10.5 (10.5)	2.9 (2.9)	3.7 (3.5)	1.1 (1.0)
τ_L-B-RMSE		10.5 (10.6)	2.7 (2.5)	4.5 (4.3)	2.1 (1.7)
u6-311 + G(2df) & ECP[d]	1.140				
τ_T-A-MAE		0.5 (0.4)	1.6 (1.6)	1.1 (1.1)	1.3 (1.3)
τ_L-A-MAE		0.5 (0.4)	1.6 (1.6)	1.1 (1.1)	1.3 (1.3)
τ_T-A-RMSE		0.7 (0.5)	2.2 (2.2)	1.4 (1.4)	1.8 (1.8)
τ_L-A-RMSE		0.7 (0.5)	2.2 (2.2)	1.4 (1.4)	1.8 (1.8)
τ_T-B-MAE		0.5 (0.5)	1.5 (1.5)	1.0 (1.0)	1.2 (1.2)
τ_L-B-MAE		0.5 (0.5)	1.5 (1.5)	1.1 (1.0)	1.2 (1.2)
τ_T-B-RMSE		0.8 (0.6)	2.1 (2.1)	1.4 (1.4)	1.7 (1.7)
τ_L-B-RMSE		0.8 (0.6)	2.1 (2.1)	1.4 (1.4)	1.7 (1.7)

[a]Entries in parenthesis are statistics for the dataset excluding two species with multireference character. [b]MAE and RMSE with relativistic correction A ($\mathcal{C}_{\mathrm{Perekls}}$) and B ($\mathcal{C}_{\mathrm{Chong}}$). [c]Average excited state $\langle\mathcal{S}^2_{\mathrm{UHF}}\rangle$ for singlets. [d]One outlier excluded for τ_T and/or τ_L.

fortuitous here as ECP calculations are generally higher than the delocalised core dataset. The projected energies are typically lower across all bases except ucc-pVTZ+ECP in the core-localised set and 6-311+G(2df) in the delocalised set. What is noteworthy is the good cost-performance of (u)6-311+G(2df) (Tables 6–7) and (u)cc-pVTZ (Tables 8–9) without breaking orbital symmetries. The method statistics for these basis sets are depicted in Tables 2–5. The overall data suggests no cost-benefit preference for the larger diffuse Dunning basis sets. In benzene, for example, the dimensions of M basis reaches beyond 400 with (u)aug-cc-pVTZ. Additional results for (u)6-311G(d) and (u)aug-cc-pVTZ can be viewed in the Supplementary Material. Finally, there appears to be very little difference in the effect of $\mathcal{C}_{\text{Perekis}}$ versus $\mathcal{C}_{\text{Chong}}$ except for the F 1s results. For the F K-edge, $\mathcal{C}_{\text{Perekis}}$ is nearly a half of an eV larger than $\mathcal{C}_{\text{Chong}}$. The smaller corrections by Chong are probably more realistic for molecules.

The first core-excitation, particularly those to orbitals of π character, do not typically require spatially expansive basis functions. Higher transitions to Rydberg orbitals, aptly described in a one-electron picture, would require at least doubly augmented diffuse functions to yield accurate energies [254]. Demonstrative calculations for the first few core-level transitions in N_2 are featured in Table 10. ΔPUMP2.5 produces viable results for these states.

4. Discussion

When applied to K-edge ionisations and excitations, the Pople basis sets augmented with additional polarisation and diffuse functions are known to offer a balance between accuracy and computational cost [255,256]. This observation is further substantiated in this work. The optimal performance u6-311+G(2df) is exemplified for ΔPUMP2.5 results with symmetry retained.

Table 3. Measure of errors w.r.t. experiment for symmetry-allowed vertical K-edge excitation energies (eV) computed with spin projection using different combinations of the 6-311 + G(2df) basis set.[a,b]

	$\langle\overline{\mathcal{S}}^2_{\text{UHF}}\rangle_{S=0}$[c]	PUHF	PUMP2	PUMP3	PUMP2.5
6 − 311 + G(2df)[d]	1.043				
τ_T-A-MAE		10.4 (10.4)	2.0 (2.0)	3.7 (3.5)	1.0 (1.0)
τ_L-A-MAE		10.4 (10.5)	1.9 (1.8)	4.2 (3.9)	1.6 (1.4)
τ_T-A-RMSE		10.8 (10.8)	2.3 (2.3)	4.1 (4.0)	1.4 (1.3)
τ_L-A-RMSE		10.8 (10.9)	2.3 (2.0)	4.8 (4.6)	2.3 (2.0)
τ_T-B-MAE		10.3 (10.2)	2.1 (2.2)	3.5 (3.4)	0.9 (0.8)
τ_L-B-MAE		10.3 (10.3)	2.0 (1.9)	4.0 (3.8)	1.4 (1.2)
τ_T-B-RMSE		10.6 (10.6)	2.4 (2.5)	4.0 (3.8)	1.2 (1.2)
τ_L-B-RMSE		10.6 (10.7)	2.4 (2.2)	4.7 (4.5)	2.2 (1.8)
6-311 + G(2df) & ECP[d]	1.139				
τ_T-A-MAE		0.6 (0.5)	1.3 (1.3)	1.0 (1.0)	1.0 (1.0)
τ_L-A-MAE		0.7 (0.6)	1.0 (1.0)	0.8 (0.8)	0.8 (0.8)
τ_T-A-RMSE		0.7 (0.6)	1.6 (1.6)	1.2 (1.2)	1.3 (1.3)
τ_L-A-RMSE		0.8 (0.7)	1.3 (1.3)	1.0 (1.0)	1.1 (1.0)
τ_T-B-MAE		0.6 (0.5)	1.2 (1.2)	0.9 (0.9)	1.0 (0.9)
τ_L-B-MAE		0.7 (0.6)	1.0 (0.9)	0.8 (0.8)	0.8 (0.8)
τ_T-B-RMSE		0.7 (0.6)	1.5 (1.5)	1.2 (1.2)	1.2 (1.2)
τ_L-B-RMSE		0.9 (0.7)	1.2 (1.2)	1.0 (1.0)	1.0 (1.0)
u6-311 + G(2df)[d]	1.039				
τ_T-A-MAE		10.2 (10.2)	2.5 (2.5)	3.4 (3.2)	0.8 (0.7)
τ_L-A-MAE		10.2 (10.3)	2.2 (2.1)	3.9 (3.7)	1.4 (1.1)
τ_T-A-RMSE		10.6 (10.6)	2.8 (2.8)	3.8 (3.7)	1.1 (1.1)
τ_L-A-RMSE		10.6 (10.7)	2.6 (2.4)	4.6 (4.4)	2.2 (1.8)
τ_T-B-MAE		10.1 (10.1)	2.6 (2.6)	3.2 (3.1)	0.7 (0.6)
τ_L-B-MAE		10.1 (10.1)	2.3 (2.2)	3.8 (3.6)	1.3 (1.0)
τ_T-B-RMSE		10.4 (10.5)	3.0 (3.0)	3.6 (3.5)	1.0 (1.0)
τ_L-B-RMSE		10.5 (10.5)	2.7 (2.5)	4.5 (4.3)	2.1 (1.7)
u6-311 + G(2df) & ECP[d]	1.140				
τ_T-A-MAE		0.7 (0.6)	1.2 (1.2)	0.9 (0.8)	1.0 (1.0)
τ_L-A-MAE		0.7 (0.6)	0.9 (0.8)	0.9 (0.8)	1.0 (1.0)
τ_T-A-RMSE		1.0 (0.8)	1.8 (1.8)	1.1 (1.1)	1.4 (1.4)
τ_L-A-RMSE		0.9 (0.8)	1.1 (1.1)	1.1 (1.1)	1.5 (1.5)
τ_T-B-MAE		0.8 (0.7)	1.1 (1.1)	0.9 (0.8)	1.0 (0.9)
τ_L-B-MAE		0.8 (0.7)	0.9 (0.8)	0.9 (0.8)	1.0 (1.0)
τ_T-B-RMSE		1.0 (0.9)	1.7 (1.8)	1.1 (1.1)	1.4 (1.4)
τ_L-B-RMSE		1.0 (0.9)	1.1 (1.1)	1.1 (1.1)	1.4 (1.4)

[a]Entries in parenthesis are statistics for the dataset excluding two species with multireference character. [b]MAE and RMSE with relativistic correction A ($\mathcal{C}_{\text{Perekis}}$) and B ($\mathcal{C}_{\text{Chong}}$). [c]Average excited state $\langle\mathcal{S}^2_{\text{UHF}}\rangle$ for singlets. [d]One outlier excluded for τ_T and/or τ_L.

Table 4. Measure of errors w.r.t. experiment for symmetry-allowed vertical K-edge excitation energies (eV) computed without spin projection using different combinations of the cc-pVTZ basis set.[a,b]

	$\langle\overline{S}^2_{UHF}\rangle_{S=0}$[c]	UHF	UMP2	UMP3	UMP2.5
cc-pVTZ[d]	1.038				
τ_T-A-MAE		10.5 (10.6)	2.2 (2.1)	3.7 (3.5)	1.0 (0.8)
τ_L-A-MAE		10.5 (10.5)	2.1 (2.0)	4.3 (4.0)	1.7 (1.5)
τ_T-A-RMSE		10.9 (11.0)	2.6 (2.5)	4.1 (3.9)	1.6 (1.3)
τ_L-A-RMSE		10.9 (10.9)	2.6 (2.4)	5.0 (4.7)	2.7 (2.3)
τ_T-B-MAE		10.4 (10.5)	2.3 (2.3)	3.5 (3.3)	1.0 (0.8)
τ_L-B-MAE		10.4 (10.4)	2.2 (2.1)	4.1 (3.9)	1.6 (1.4)
τ_T-B-RMSE		10.7 (10.8)	2.8 (2.7)	3.9 (3.7)	1.5 (1.2)
τ_L-B-RMSE		10.7 (10.7)	2.7 (2.5)	4.9 (4.5)	2.6 (2.2)
cc-pVTZ & ECP[d]	1.138				
τ_T-A-MAE		0.7 (0.6)	2.4 (2.4)	1.9 (2.0)	2.2 (2.2)
τ_L-A-MAE		0.7 (0.6)	2.4 (2.4)	2.0 (2.0)	2.2 (2.2)
τ_T-A-RMSE		0.9 (0.8)	2.7 (2.7)	2.2 (2.2)	2.4 (2.4)
τ_L-A-RMSE		0.9 (0.8)	2.7 (2.7)	2.2 (2.2)	2.5 (2.5)
τ_T-B-MAE		0.6 (0.6)	2.3 (2.2)	1.8 (1.8)	2.0 (2.0)
τ_L-B-MAE		0.6 (0.6)	2.3 (2.6)	1.8 (1.8)	2.1 (2.1)
τ_T-B-RMSE		0.9 (0.8)	2.5 (2.5)	2.1 (2.1)	2.3 (2.3)
τ_L-B-RMSE		0.9 (0.8)	2.3 (2.6)	2.1 (2.1)	2.3 (2.3)
ucc-pVTZ[d]	1.039				
τ_T-A-MAE		10.5 (10.6)	2.3 (2.3)	3.7 (3.5)	1.0 (0.8)
τ_L-A-MAE		10.5 (10.6)	2.3 (2.2)	4.3 (4.1)	1.6 (1.5)
τ_T-A-RMSE		11.0 (11.1)	2.8 (2.7)	4.2 (4.0)	1.7 (1.4)
τ_L-A-RMSE		11.0 (11.1)	2.7 (2.5)	5.1 (5.0)	2.7 (2.5)
τ_T-B-MAE		10.4 (10.5)	2.5 (2.4)	3.5 (3.3)	1.0 (0.8)
τ_L-B-MAE		10.4 (10.5)	2.4 (2.3)	4.1 (3.9)	1.6 (1.4)
τ_T-B-RMSE		10.8 (10.9)	2.9 (2.8)	4.1 (3.9)	1.6 (1.3)
τ_L-B-RMSE		10.8 (10.9)	2.8 (2.6)	4.9 (4.8)	2.6 (2.4)
ucc-pVTZ & ECP[d]	1.137				
τ_T-A-MAE		0.6 (0.5)	1.6 (1.6)	1.9 (1.9)	1.7 (1.7)
τ_L-A-MAE		0.6 (0.5)	1.6 (1.6)	1.9 (2.0)	1.7 (1.7)
τ_T-A-RMSE		0.8 (0.7)	2.1 (2.1)	2.2 (2.2)	2.0 (2.1)
τ_L-A-RMSE		0.8 (0.7)	2.2 (2.2)	2.3 (2.3)	2.1 (2.2)
τ_T-B-MAE		0.6 (0.5)	1.5 (1.5)	1.7 (1.8)	1.5 (1.5)
τ_L-B-MAE		0.6 (0.5)	1.6 (1.5)	1.8 (1.8)	1.6 (1.6)
τ_T-B-RMSE		0.9 (0.8)	2.0 (2.0)	2.1 (2.1)	1.9 (1.9)
τ_L-B-RMSE		0.9 (0.8)	2.1 (2.1)	2.2 (2.2)	2.0 (2.0)

[a]Entries in parenthesis are statistics for the dataset excluding two species with multireference character. [b]MAE and RMSE with relativistic correction A ($\mathcal{C}_{\text{Perekls}}$) and B ($\mathcal{C}_{\text{Chong}}$). [c]Average excited state $\langle\mathcal{S}^2_{UHF}\rangle$ for singlets. [d]One outlier excluded for τ_T and/or τ_L.

Core-localised ΔPUHF results are sufficient with (u)6-311+G(2df)+ECP. Other basis sets designed for improved core orbitals could have be chosen [257]. Instead, we sought to examine the effect of decontracting standard basis sets.

The ΔPUMP2.5 method for estimating vertical excitation energies can reach sub-electron-volt accuracy when orbital symmetry is preserved. This result is very useful since spin, ORX, and quasi-extrapolated correlation corrections are accounted for in the model. The validity of ΔSCF is also once again apparent for when one adopts a localised picture of core orbitals. To ensure that energies correspond to states with good spin quantum numbers, spin projection is necessary if the UHF wavefunction breaks symmetry. For chemical species with ground state multireference character, such as C_2 and O_3, single determinant ΔSCF methods are normally inadequate. In this study, notable deviations of ΔPUHF from experiment for these molecules is observed. However, other single configuration methods can be applied to the core excited states of O_3, since the multireference character of the ground state may not necessarily translate into the core excited state [258]. Additionally, when molecules undergo an adiabatic transition, the vertical ω_X values will normally be larger than what is observed. In the assortment of molecules selected, allene and CO_2 experience Jahn-Teller/Renner-Teller distortions, [259,260] so vertical ω_X values for the principle transition are also expected to be less accurate. Transitions associated with fine vibrational structure in core spectra are not accounted for either.

The mixed portrait of ORX and correlation inherent in a localised core-hole reference makes ΔSCF a satisfactory approach, especially for molecules with nonequivalent, asymmetrical atomic sites. The parallel approach of delegating the labor of modelling ORX to ΔSCF and separately recovering correlations through $n = 2$, 3 or 2.5 order MP perturbation theory is also a theoretically

Table 5. Measure of errors w.r.t. experiment for symmetry-allowed vertical K-edge excitation energies (eV) computed with spin projection using different combinations of the cc-pVTZ basis set.[a,b]

	$\langle \overline{\mathcal{S}}^2_{\mathrm{UHF}} \rangle_{S=0}$[c]	PUHF	PUMP2	PUMP3	PUMP2.5
cc-pVTZ[d]	1.038				
τ_T-A-MAE		10.5 (10.6)	2.2 (2.1)	3.6 (3.4)	1.0 (0.8)
τ_L-A-MAE		10.5 (10.5)	2.1 (2.0)	4.3 (4.0)	1.7 (1.4)
τ_T-A-RMSE		10.9 (11.0)	2.6 (2.5)	4.1 (3.8)	1.6 (1.2)
τ_L-A-RMSE		10.9 (10.9)	2.6 (2.4)	5.0 (4.7)	2.7 (2.3)
τ_T-B-MAE		10.4 (10.4)	2.4 (2.3)	3.5 (3.3)	0.9 (0.7)
τ_L-B-MAE		10.4 (10.3)	2.2 (2.1)	4.1 (3.8)	1.5 (1.3)
τ_T-B-RMSE		10.7 (10.8)	2.8 (2.7)	3.9 (3.7)	1.5 (1.1)
τ_L-B-RMSE		10.7 (10.7)	2.7 (2.5)	4.9 (4.5)	2.6 (2.2)
cc-pVTZ & ECP[d]	1.138				
τ_T-A-MAE		0.7 (0.7)	2.0 (2.0)	1.6 (1.6)	1.8 (1.8)
τ_L-A-MAE		0.7 (0.7)	2.0 (2.0)	1.6 (1.7)	1.8 (1.8)
τ_T-A-RMSE		1.0 (0.8)	2.3 (2.3)	1.9 (1.9)	2.1 (2.1)
τ_L-A-RMSE		1.0 (0.8)	2.3 (2.4)	1.9 (2.0)	2.1 (2.2)
τ_T-B-MAE		0.8 (0.7)	1.9 (2.2)	1.5 (1.5)	1.7 (1.7)
τ_L-B-MAE		0.8 (0.7)	1.9 (1.9)	1.5 (1.5)	1.7 (1.7)
τ_T-B-RMSE		1.0 (0.9)	1.9 (2.2)	1.8 (1.8)	2.0 (2.0
τ_L-B-RMSE		1.0 (0.9)	2.2 (2.2)	1.8 (1.8)	2.0 (2.0)
ucc-pVTZ[d]	1.039				
τ_T-A-MAE		10.5 (10.6)	2.4 (2.3)	3.6 (3.4)	1.0 (0.8)
τ_L-A-MAE		10.5 (10.6)	2.3 (2.2)	4.2 (4.0)	1.6 (1.4)
τ_T-A-RMSE		10.9 (11.1)	2.8 (2.7)	4.2 (4.0)	1.7 (1.3)
τ_L-A-RMSE		11.0 (11.1)	2.7 (2.5)	5.1 (5.0)	2.7 (2.4)
τ_T-B-MAE		10.4 (10.4)	2.5 (2.4)	3.5 (3.3)	1.0 (0.8)
τ_L-B-MAE		10.4 (10.4)	2.4 (2.3)	4.1 (3.9)	1.5 (1.3)
τ_T-B-RMSE		10.8 (10.9)	2.9 (2.8)	4.1 (3.9)	1.6 (1.3)
τ_L-B-RMSE		10.8 (10.9)	2.8 (2.6)	5.0 (4.8)	2.6 (2.3)
ucc-pVTZ & ECP[d]	1.137				
τ_T-A-MAE		0.8 (0.7)	2.0 (2.0)	1.6 (1.6)	1.8 (1.8)
τ_L-A-MAE		0.8 (0.7)	2.0 (2.0)	1.6 (1.6)	1.8 (1.8)
τ_T-A-RMSE		1.0 (0.9)	2.3 (2.3)	1.9 (1.9)	2.1 (2.1)
τ_L-A-RMSE		1.0 (0.9)	2.4 (2.4)	2.0 (2.0)	2.2 (2.2)
τ_T-B-MAE		0.8 (0.7)	1.8 (1.8)	1.4 (1.8)	1.6 (1.6)
τ_L-B-MAE		0.8 (0.7)	1.9 (1.9)	1.5 (1.5)	1.7 (1.7)
τ_T-B-RMSE		1.1 (0.9)	2.2 (2.2)	1.4 (1.8)	2.0 (2.0)
τ_L-B-RMSE		1.1 (0.9)	2.2 (2.2)	1.9 (1.9)	2.0 (2.1)

[a]Entries in parenthesis are statistics for the dataset excluding two species with multireference character. [b]MAE and RMSE with relativistic correction A ($\mathcal{C}_{\mathrm{Perekls}}$) and B ($\mathcal{C}_{\mathrm{Chong}}$). [c]Average excited state $\langle \mathcal{S}^2_{\mathrm{UHF}} \rangle$ for singlets. [d]One outlier excluded for τ_T and/or τ_L.

sound model for symmetrical molecules. Preserving the orbital symmetry and applying the latter method would assist with spectral assignments. One can also break symmetry, use ΔSCF, and rely on visual inspection of the orbitals involved if the spatial character of said orbitals are known *a priori*. In both approaches, spin projection is necessary for obtaining an approximately right answer for the right reason.

Although the quantum chemistry problem is established clearly and addressed quite well with the methods introduced, there are numerical complications and idiosyncrasies that accompany the use of single determinant core-hole with perturbation theory. The issues are delineated as follows:

(1) The PUHF and PUMP*n* variants employed here involve PAV, so the projected energies and wavefunctions do not necessarily correspond to a proper eigenstate of $\mathcal{H}$. Alternatively, VAP spin projection methods can be applied for locating PUHF stationary states along with extensions thereof to include dynamic correlation [261,262].

(2) The monodeterminantal non-Aufbau reference is not an excited state wavefunction that transforms under the proper molecular electronic symmetry operations. It is an SCF solution that can only provide a representative charge density that, in principle, corresponds to a single target non-Aufbau configuration. With solutions found with guided SCF solvers (e.g. MOM), there is no guarantee the particle-hole pair orbitals will resemble the ones of the ground state. The SCF orbital optimisation process will attempt to converge any solution given the overlap metric or level-shifting directive. The core-hole solution may then give a meaningful energy with respect to the ground state, but its core-hole and/or newly occupied valence orbitals may be distorted. A deformed core-hole density can lead to

Table 6. Vertical *K*-edge excitation energies (eV) using u6-311+G(2df) without spin projection.[a]

Molecule	K-Edge	UHF	UMP2	UMP3	UMP2.5	Exp.
N_2	N	409.7	397.6	403.5	400.5	400.9 [224]
cis-Diazene	N	407.6	396.1	400.5	398.3	398.4 [227]
C_2H_2	C	293.4	283.9	287.3	285.6	285.9 [223]
C_2H_4	C	292.5	283.6	285.7	284.7	284.7 [223]
C_2H_6	C	294.8	285.5	287.9	286.7	286.9 [223]
F_2	F	694.1	678.3	684.8	681.5	682.2 [226]
O_3 (**O** = O–O)	O	540.0	525.7	533.6	529.6	529.1 [225]
H_2O_2	O	543.8	529.4	535.6	532.5	533.0 [228]
CO_2	O	546.5	531.8	540.0	535.9	535.4 [231]
O_2	O	542.0	526.8	534.2	530.5	530.8 [234]
C_2N_2	C	293.6	286.2	287.8	287.0	286.3 [230]
C_2N_2	N	409.8	393.1	403.5	398.3	398.9 [230]
Cyclopropane	C	295.4	285.9	288.7	287.3	287.7 [235]
C_2F_4	C	297.9	293.2	294.2	293.7	290.1 [229]
C_2F_4	F	708.6	685.1	697.2	691.2	690.7 [229]
CF_2O	F	701.0	688.2	694.7	691.4	689.2 [232]
CH_2CF_2	F	701.5	687.8	694.4	691.1	690.3 [229]
cis-CH_2CF_2	F	700.9	685.3	692.4	688.9	689.3 [229]
Hydrazine	N	411.4	399.0	404.0	401.5	401.5 [233]
Furan (**C**–O)	C	295.3	285.3	289.0	287.2	286.6 [238]
OF_2	F	696.6	680.1	688.9	684.5	683.8 [237]
Urea	N	411.9	400.4	406.0	403.2	402.0 [236]
N_3^- (**N** = N = N)	N	410.3	394.4	405.5	399.9	399.6 [227]
Allene (**C** = C = C)	C	286.8	286.6	286.5	286.6	285.4 [242]
Cyclobutane	C	299.3	286.0	288.4	287.2	287.4 [235]
C_2	C	295.4	284.3	292.1	288.2	285.9 [223,243]
Acetone (**C**–C = O)	C	295.8	286.0	289.3	287.6	288.4 [244]
Pyridine (**C**–N)	C	294.4	283.8	288.0	285.9	285.3 [240]
Tetrazine	C	295.0	284.2	289.0	286.6	285.2 [239]
Tetrazine	N	413.1	396.6	404.1	400.3	398.8 [239,240]
Benzene	C	297.6	283.2	286.9	285.0	285.2 [245]
Pyrrole (**C**–NH)	C	295.2	284.7	288.7	286.7	286.3 [246]
NF_3	F	700.6	684.3	692.7	688.5	687.4 [241]

[a]Results using τ_T and $\mathcal{C}_{\text{Chong}}$.

Table 7. Vertical *K*-edge excitation energies (eV) using u6-311+G(2df) with spin projection.[a]

Molecule	K-Edge	PUHF	PUMP2	PUMP3	PUMP2.5	Exp.
N_2	N	410.0	397.9	403.8	400.8	400.9 [224]
cis-Diazene	N	407.9	396.3	400.8	398.5	398.4 [227]
C_2H_2	C	293.5	284.0	287.4	285.7	285.9 [223]
C_2H_4	C	292.6	283.7	285.9	284.8	284.7 [223]
C_2H_6	C	294.7	285.4	287.8	286.6	286.9 [223]
F_2	F	694.7	678.9	685.4	682.2	682.2 [226]
O_3 (**O** = O–O)	O	539.9	525.5	533.4	529.4	529.1 [225]
H_2O_2	O	544.3	530.0	536.1	533.0	533.0 [228]
CO_2	O	546.5	531.8	540.0	535.9	535.4 [231]
O_2	O	541.9	526.7	534.2	530.5	530.8 [234]
C_2N_2	C	292.9	285.5	287.1	286.3	286.3 [230]
C_2N_2	N	409.7	393.0	403.4	398.2	398.9 [230]
Cyclopropane	C	295.3	285.8	288.6	287.2	287.7 [235]
C_2F_4	C	298.2	293.5	294.5	294.0	290.1 [229]
C_2F_4	F	708.4	685.0	697.1	691.0	690.7 [229]
CF_2O	F	700.9	688.0	694.5	691.2	689.2 [232]
CH_2CF_2	F	701.3	687.5	694.2	690.8	690.3 [229]
cis-CH_2CF_2	F	700.8	685.2	692.2	688.7	689.3 [229]
Hydrazine	N	411.4	398.9	403.9	401.4	401.5 [233]
Furan (**C**–O)	C	295.3	285.3	289.0	287.1	286.6 [238]
OF_2	F	696.8	680.2	689.0	684.6	683.8 [237]
Urea	N	411.9	400.4	406.0	403.2	402.0 [236]
N_3^- (**N** = N = N)	N	410.2	394.2	405.3	399.8	399.6 [227]
Allene (**C** = C = C)	C	286.4	286.2	286.1	286.1	285.4 [242]
Cyclobutane	C	299.2	285.9	288.3	287.1	287.4 [235]
C_2	C	295.6	284.5	292.3	288.4	285.9 [223,243]
Acetone (**C**–C = O)	C	295.7	285.9	289.2	287.5	288.4 [244]
Pyridine (**C**–N)	C	294.1	283.5	287.7	285.6	285.3 [240]
Tetrazine	C	295.0	284.2	289.0	286.6	285.2 [239]
Tetrazine	N	412.9	396.4	403.9	400.2	398.8 [239,240]
Benzene	C	297.4	283.0	286.7	284.8	285.2 [245]
Pyrrole (**C**–NH)	C	295.2	284.6	288.7	286.7	286.3 [246]
NF_3	F	700.7	684.4	692.8	688.6	687.4 [241]

[a]Results using τ_T and $\mathcal{C}_{\text{Chong}}$.

Table 8. Vertical *K*-edge excitation energies (eV) using ucc-pVTZ without spin projection.[a]

Molecule	K-Edge	UHF	UMP2	UMP3	UMP2.5	Exp.
N_2	N	409.7	397.6	403.4	400.5	400.9 [224]
cis-Diazene	N	407.6	396.1	400.5	398.3	398.4 [227]
C_2H_2	C	293.4	284.0	287.3	285.7	285.9 [223]
C_2H_4	C	292.4	283.7	285.8	284.7	284.7 [223]
C_2H_6	C	295.5	286.2	288.6	287.4	286.9 [223]
F_2	F	694.2	678.5	684.8	681.6	682.2 [226]
O_3 (**O** = O–O)	O	540.1	525.8	533.5	529.7	529.1 [225]
H_2O_2	O	543.8	529.6	535.6	532.6	533.0 [228]
CO_2	O	546.5	531.8	540.1	535.9	535.4 [231]
O_2	O	542.0	526.9	534.2	530.5	530.8 [234]
C_2N_2	C	293.6	286.0	287.6	286.8	286.3 [230]
C_2N_2	N	409.8	394.7	404.8	399.7	398.9 [230]
Cyclopropane	C	296.1	286.3	289.3	287.8	287.7 [235]
C_2F_4	C	297.9	294.9	296.4	295.6	290.1 [229]
C_2F_4	F	708.6	683.9	695.8	689.9	690.7 [229]
CF_2O	F	701.2	688.6	694.5	691.6	689.2 [232]
CH_2CF_2	F	701.6	686.8	693.5	690.2	690.3 [229]
cis-CH_2CF_2	F	700.9	685.3	692.3	688.8	689.3 [229]
Hydrazine	N	411.7	399.2	404.3	401.7	401.5 [233]
Furan (**C**–O)	C	295.3	285.3	289.0	287.1	286.6 [238]
OF_2	F	696.7	680.3	688.9	684.6	683.8 [237]
Urea	N	412.5	402.7	407.8	405.3	402.0 [236]
N_3^- (**N** = N = N)	N	410.3	394.8	405.1	400.0	399.6 [227]
Allene (**C** = C = C)	C	286.9	286.7	286.6	286.6	285.4 [242]
Cyclobutane	C	300.3	286.6	289.3	287.9	287.4 [235]
C_2	C	295.4	284.4	292.1	288.2	285.9 [223,243]
Acetone (**C**–C = O)	C	296.5	285.8	289.2	287.5	288.4 [244]
Pyridine (**C**–N)	C	294.4	283.7	287.9	285.8	285.3 [240]
Tetrazine	C	295.0	283.6	288.4	286.0	285.2 [239]
Tetrazine	N	413.1	399.2	406.3	402.7	398.8 [239,240]
Benzene	C	297.5	283.2	287.0	285.1	285.2 [245]
Pyrrole (**C**–NH)	C	295.3	284.6	288.6	286.6	286.3 [246]
NF_3	F	705.4	684.5	696.6	690.5	687.4 [241]

[a]Results using τ_T and C_{Chong}.

poor ΔMP energies and loss of an intuitive molecular orbital picture. We encounter this problem with many molecules for calculations using some basis sets in tandem with ECPs. At times, these 'excited-state' solutions can only converge with basis set projections from other calculations. This situation can give rise to multiple SCF solutions with similar energies that are difficult to distinguish by orbital shape and occupation. Nonetheless, ΔSCF + ECP results still yield viable estimates of core-excitation energies.

(3) The use of the MWB2 ECPs seems to interfere with the correlation consistency of the Dunning basis, so different pseudopotentials could prove to be more viable [263]. Another possibility is to apply the Edmiston-Ruedenberg [264] or Boys [265] localisation to break the core orbital symmetry. Localisation lacks the advantage ECPs have for reducing the number of non-target occupied core orbitals that may contribute to occurrence of small denominators and the number of occupied orbitals included in the correlation window.

(4) The convergence behaviour of the MP series is mainly understood for ground state references. For references other than the ground state, it is less predictable [266,267]. The most prominent errors in the perturbative calculations with core-hole references comes from (a) divergence in MP3 and (b) different orbital correlation windows between the ground and excited states due to index freezing. Orbitals indices are only frozen in the core excited-state to mitigate the small denominators. Divergence at third-order may be avoided, but the correlation corrections are not summed over the same indices of the ground state. This leads to an imbalanced treatment of correlation. These errors are most pronounced in the ω_X computed with ΔMP3 and ΔMP2.5 as the third-order correction is not stable. Often, the presence of basis sets with higher angular momentum functions or nearly degenerate orbitals eventually lead to a greater amount of frozen indices. The tighter threshold τ_T reduces this amount and improves the energies but, in some cases, $\sim 40-60\%$ of the orbital window remains frozen. This problem doesn't appear to scale with the size of the molecule, as benzene with uaug-cc-pVTZ required just two orbitals to be removed at τ_L. With the approach taken here, it is unclear how to maintain a 1:1 mapping between ground and excited SCF orbitals when significant relaxation that occurs. To aid in identifying orbitals to correlate, perhaps a

Table 9. Vertical *K*-edge excitation energies (eV) using ucc-pVTZ with spin projection.[a]

Molecule	K-Edge	UHF	UMP2	UMP3	UMP2.5	Exp.
N_2	N	410.0	397.9	403.7	400.8	400.9 [224]
cis-Diazene	N	407.9	396.4	400.7	398.5	398.4 [227]
C_2H_2	C	293.5	284.1	287.4	285.8	285.9 [223]
C_2H_4	C	292.5	283.8	285.9	284.8	284.7 [223]
C_2H_6	C	295.4	286.1	288.5	287.3	286.9 [223]
F_2	F	694.8	679.1	685.4	682.3	682.2 [226]
O_3 (**O** = O–O)	O	539.9	525.6	533.3	529.5	529.1 [225]
H_2O_2	O	544.3	530.1	536.1	533.1	533.0 [228]
CO_2	O	546.5	531.8	540.0	535.9	535.4 [231]
O_2	O	542.0	526.8	534.2	530.5	530.8 [234]
C_2N_2	C	292.9	285.2	286.8	286.0	286.3 [230]
C_2N_2	N	409.9	394.7	404.8	399.8	398.9 [230]
Cyclopropane	C	296.0	286.2	289.2	287.7	287.7 [235]
C_2F_4	C	298.2	295.2	296.7	296.0	290.1 [229]
C_2F_4	F	708.4	683.7	695.6	689.6	690.7 [229]
CF_2O	F	701.0	688.5	694.4	691.4	689.2 [232]
CH_2CF_2	F	701.5	686.7	693.3	690.0	690.3 [229]
cis-CH_2CF_2	F	700.7	685.1	692.0	688.6	689.3 [229]
Hydrazine	N	411.6	399.2	404.2	401.7	401.5 [233]
Furan (**C**–O)	C	295.3	285.3	289.0	287.1	286.6 [238]
OF_2	F	696.9	680.5	689.1	684.8	683.8 [237]
Urea	N	412.5	402.8	407.9	405.3	402.0 [236]
N_3^- (**N** = N = N)	N	410.2	394.7	405.0	399.8	399.6 [227]
Allene (**C** = C = C)	C	286.4	286.2	286.2	286.2	285.4 [242]
Cyclobutane	C	300.2	286.5	289.2	287.8	287.4 [235]
C_2	C	295.6	284.6	292.3	288.4	285.9 [223,243]
Acetone (**C**–C = O)	C	296.4	285.7	289.1	287.4	288.4 [244]
Pyridine (**C**–N)	C	294.0	283.3	287.5	285.4	285.3 [240]
Tetrazine	C	295.1	283.6	288.4	286.0	285.2 [239]
Tetrazine	N	413.0	399.0	406.1	402.6	398.8 [239,240]
Benzene	C	297.3	283.0	286.8	284.9	285.2 [245]
Pyrrole (**C**–NH)	C	295.2	284.5	288.5	286.5	286.3 [246]
NF_3	F	705.3	684.5	696.6	690.5	687.4 [241]

[a]Results using τ_T and C_{Chong}.

Table 10. Core-level valence and Rydberg transitions (eV) of N_2.[a]

State	Excitation	PUHF	PUMP2	PUMP3	PUMP2.5	Exp.[c]	Exp.[d]
$^1\Pi_u$	$(1s\sigma_u^{-1})(2p\pi_g)^1$	410.0[b]	397.8	403.6	400.9	400.9	400.8
$^1\Sigma_u^+$	$(1s\sigma_u^{-1})(3s\sigma_g)^1$	415.7	400.9	410.8	406.0	406.2	405.6
$^1\Pi_u$	$(1s\sigma_g^{-1})(3p\pi_u)^1$	416.6	401.8	411.8	407.0	407.1	406.5
$^1\Sigma_u^+$	$(1s\sigma_g^{-1})(3p\sigma_u)^1$	416.8	402.0	412.1	407.2	407.3	406.7
	K-Edge IP	419.1	404.6	414.4	409.7	409.9	409.5

[a]udaug-cc-pVTZ, C_{Chong}, full orbital window. [b]Up-projected from ucc-pVTZ. [c]Ref. [251] [d]Refs. [252,253]

reduced set of compact, local virtual orbitals can be found and passed to the ground and excited state MP calculations.

In the context of CC and MP calculations, thorough assessments of related schemes show how contributions from amplitudes involving the virtual core orbital can be modulated to resolve the 'dangerous' denominator problem [92,93,100]. For example, Arias-Martinez et al. demonstrate that ΔCCSD results with configuration-based denominator control can become competitive with ΔSCF [93]. Theses schemes also exhibit more stable convergence behaviour with basis sets of increasing cardinal number. Thus, for post-SCF methods, such protocols are likely preferred over filtering correlation terms based on simple denominator-sum thresholds.

Conventional implementations of projected MP can be cost-prohibitive for very large molecules. Density-fitting or resolution of the identity methods could be used to accelerate the evaluation of UMP*n* contributions to the projected energy [268,269]. Although the methods are well-grounded for single reference molecules, the results in this study have proven to be very sensitive to calculation setup details such as the choice and quality of the reference determinant and protocols for incorporating perturbative corrections.

5. Conclusions

Vertical core-excitation energies at the C, N, O, and F *K*-edge are obtained with ΔPUHF and ΔPUMP*n* for a set of symmetrical molecules with equivalent atoms. The

methods employed inherit old quantum chemistry concepts for modelling the electronic structure of core-holes. The historical foundations of the validity and efficiency of ΔSCF with core-localisation is reaffirmed. Second-order Møller–Plesset perturbation theory recovers a large fraction of the missing correlation in ΔSCF for molecules with equivalent atomic sites. Averaged corrections from PUMP2 and PUMP3 combined with PUHF, for a select assortment of basis sets, provides the best performance when molecular symmetry is present.

The results are heavily influenced by the quality of the SCF solutions and the number of indices removed to avoid divergences in the MP energies. The effect of the scalar relativistic corrections incorporated in this work on the overall statistics do not vary between corrections schemes except in F 1s excitations. The relativistic IP shift in the two-electron atomic model is too high for F and atoms with higher Z. For the K-edge ω_X values computed here, C_{Chong} is preferred. A more complete relativistic description of molecules with heavier atoms is also needed. Additionally, single reference Δ-based approaches would require proper addition of spin-orbit effects to be applicable to L-edge calculations due to degeneracy and multiplet structure of the final states [71,132].

Nevertheless, for an excitation defined by a canonical particle-hole pair, the quantitative performance of ΔPMP2.5 or ΔPUHF limits the need for significant empirical shifting. Step-wise reproduction and assignment of spectra is achievable provided transition dipole strengths are obtained using the projected UHF or PUMP density corrections. Data from each calculation could be concatenated to generate the spectra up to the IP. Auger cascading and shake-related processes involve the correlated, physical motion of two- or many- electrons not described in single configuration mean-field theory. One must then turn to more accurate methods that contain information on the two-particle density matrix and Feynman-Dyson amplitudes for computing energies and transition strengths [270,271].

Acknowledgments

We thank Professor H. B. Schlegel for helpful and informative discussions related to some of the methods applied in this paper.

Disclosure statement

No potential conflict of interest was reported by the author(s).

Data availability statement

The data that support the findings of this study are available within the article and its supplementary material.

Funding

This research was supported by the National Science Foundation (Award CHE-1848580). Computational resources were provided by the Pinnacles cluster at UC Merced, which is also supported by the National Science Foundation (Award OAC-2019144).

References

[1] A. Hitchcock, Ultramicroscopy **28** (1), 165–183 (1989). doi:10.1016/0304-3991(89)90290-8
[2] A.P. Hitchcock, Phys. Scr. **1990** (T31), 159 (1990). doi:10.1088/0031-8949/1990/T31/023
[3] P.M. Kraus, M. Zürch, S.K. Cushing, D.M. Neumark and S.R. Leone, Nat. Rev. Chem. **2** (6), 82–94 (2018). doi:10.1038/s41570-018-0008-8
[4] L.X. Chen, X. Zhang and M.L. Shelby, Chem. Sci. **5** (11), 4136–4152 (2014). doi:10.1039/C4SC01333F
[5] C. Bressler and M. Chergui, Chem. Rev. **104** (4), 1781–1812 (2004). doi:10.1021/cr0206667
[6] C. Bressler and M. Chergui, Annu. Rev. Phys. Chem. **61** (1), 263–282 (2010). doi:10.1146/physchem.2010.61.issue-1
[7] F. de Groot, Chem. Rev. **101** (6), 1779–1808 (2001). doi:10.1021/cr9900681
[8] A.P. Hitchcock, Jpn. J. Appl. Phys. **32** (S2), 176 (1993). doi:10.7567/JJAPS.32S2.176
[9] M. Chergui and E. Collet, Chem. Rev. **117** (16), 11025–11065 (2017). doi:10.1021/acs.chemrev.6b00831
[10] L. Young, K. Ueda, M. Gühr, P.H. Bucksbaum, M. Simon, S. Mukamel, N. Rohringer, K.C. Prince, C. Masciovecchio, M. Meyer, A. Rudenko, D. Rolles, C. Bostedt, M. Fuchs, D.A. Reis, R. Santra, H. Kapteyn, M. Murnane, H. Ibrahim, F. Légaré, M. Vrakking, M. Isinger, D. Kroon, M. Gisselbrecht, A. L'Huillier, H.J. Wörner and S.R. Leone, J. Phys. B: At. Mol. Phys. **51** (3), 032003 (2018). doi:10.1088/1361-6455/aa9735
[11] R. Geneaux, H.J.B. Marroux, A. Guggenmos, D.M. Neumark and S.R. Leone, Philos. Trans. R. Soc. A **377** (2145), 20170463 (2019). doi:10.1098/rsta.2017.0463
[12] K.J. Gaffney, Chem. Sci. **12** (23), 8010–8025 (2021). doi:10.1039/D1SC01864G
[13] A.R. Attar, H.T. Chang, A. Britz, X. Zhang, M.F. Lin, A. Krishnamoorthy, T. Linker, D. Fritz, D.M. Neumark, R.K. Kalia, A. Nakano, P. Ajayan, P. Vashishta, U. Bergmann and S.R. Leone, ACS Nano**14** (11), 15829–15840 (2020). doi:10.1021/acsnano.0c06988
[14] P. Ghigna and E. Quartarone, J. Phys. Energy **3** (3), 032006 (2021). doi:10.1088/2515-7655/abf2db
[15] K.F. Chang, M. Reduzzi, H. Wang, S.M. Poullain, Y. Kobayashi, L. Barreau, D. Prendergast, D.M. Neumark and S.R. Leone, Nat. Commun. **11** (1), 4042 (2020). doi: 10.1038/s41467-020-17745-w
[16] B. Stankus, H. Yong, J. Ruddock, L. Ma, A.M. Carrascosa, N. Goff, S. Boutet, X. Xu, N. Zotev, A. Kirrander, M.P. Minitti and P.M. Weber, J. Phys. B: At. Mol. Phys. **53** (23), 234004 (2020). doi:10.1088/1361-6455/abbfea
[17] C.D. Rankine and T.J. Penfold, J. Phys. Chem. A **125** (20), 4276–4293 (2021). doi:10.1021/acs.jpca.0c11267
[18] D.A. Chin, P.M. Nilson, D. Mastrosimone, D. Guy, J.J. Ruby, D.T. Bishel, J.F. Seely, F. Coppari, Y. Ping, J.R.

Rygg and G.W. Collins, Rev. Sci. Instrum. **94** (1), 013101 (2023). doi:10.1063/5.0125712
[19] J.S. Kaastra, Astron. Nachr. **338** (2-3), 146–152 (2017). doi:10.1002/asna.v338.2/3
[20] J. Duris, S. Li, T. Driver, E.G. Champenois, J.P. MacArthur, A.A. Lutman, Z. Zhang, P. Rosenberger, J.W. Aldrich, R. Coffee, G. Coslovich, F.J. Decker, J.M. Glownia, G. Hartmann, W. Helml, A. Kamalov, J. Knurr, J. Krzywinski, M.F. Lin, J.P. Marangos, M. Nantel, A. Natan, J.T. O'Neal, N. Shivaram, P. Walter, A.L. Wang, J.J. Welch, T.J.A. Wolf, J.Z. Xu, M.F. Kling, P.H. Bucksbaum, A. Zholents, Z. Huang, J.P. Cryan and A. Marinelli, Nat. Photonics **14** (1), 30–36 (2019). doi:10.1038/s41566-019-0549-5
[21] A.G. Shard, J. Vac. Sci. Technol. A **38** (4), 041201 (2020). doi:10.1116/1.5141395
[22] T. Papp and J. Maxwell, X-Ray Spectrom. **46** (5), 367–373 (2017). doi:10.1002/xrs.v46.5
[23] G.S. Wojcik, J. Res. Natl. Inst. Stand. Technol. **109** (5), 479 (2004). doi:10.6028/jres
[24] O. Sublemontier, C. Nicolas, D. Aureau, M. Patanen, H. Kintz, X. Liu, M.A. Gaveau, J.L. Le Garrec, E. Robert, F.A. Barreda, A. Etcheberry, C. Reynaud, J.B. Mitchell and C. Miron, J. Phys. Chem. Lett. **5** (19), 3399–3403 (2014). doi:10.1021/jz501532c
[25] F. de Groot, G. Vankó and P. Glatzel, J. Phys. Condens. Matter **21** (10), 104207 (2009). doi:10.1088/0953-8984/21/10/104207
[26] D.G.J. Sutherland, M. Kasrai, G.M. Bancroft, Z.F. Liu and K.H. Tan, Phys. Rev. B **48**, 14989–15001 (1993). doi:10.1103/PhysRevB.48.14989
[27] C.J. Pollock and S. DeBeer, Acc. Chem. Res. **48** (11), 2967–2975 (2015). doi:10.1021/acs.accounts.5b00309
[28] P. Norman and A. Dreuw, Chem. Rev. **118** (15), 7208–7248 (2018). doi:10.1021/acs.chemrev.8b00156
[29] K. Mathew, C. Zheng, D. Winston, C. Chen, A. Dozier, J.J. Rehr, S.P. Ong and K.A. Persson, Sci. Data **5** (1), 180151 (2018). doi:10.1038/sdata.2018.151
[30] J.A. Van Bokhoven and C. Lamberti, *X-Ray Absorption and X-Ray Emission Spectroscopy: Theory and Applications*, Vol. 1. (John Wiley & Sons, 2016).
[31] T. Fransson, Y. Harada, N. Kosugi, N.A. Besley, B. Winter, J.J. Rehr, L.G.M. Pettersson and A. Nilsson, Chem. Rev. **116** (13), 7551–7569 (2016). doi:10.1021/acs.chemrev.5b00672
[32] P.S. Bagus, E.S. Ilton and C.J. Nelin, Surf. Sci. Rep. **68** (2), 273–304 (2013). doi:10.1016/j.surfrep.2013.03.001
[33] P.S. Bagus, F. Illas, G. Pacchioni and F. Parmigiani, J. Electron. Spectrosc. Relat. Phenom. **100** (1), 215–236 (1999). doi:10.1016/S0368-2048(99)00048-1
[34] F. de Groot, J. Electron. Spectrosc. Relat. Phenom. **62** (1), 111–130 (1993). doi:10.1016/0368-2048(93)80009-B
[35] J.M. Kasper, T.F. Stetina, A.J. Jenkins and X. Li, Chem. Phys. Rev. **1** (1), 011304 (2020). doi:10.1063/5.0029725
[36] N.A. Besley, Wiley Interdiscip. Rev.: Comput. Mol. Sci. **11** (6), e1527 (2021).
[37] C.C.J. Roothaan, Rev. Mod. Phys. **23**, 69–89 (1951). doi:10.1103/RevModPhys.23.69
[38] P.S. Bagus, Phys. Rev. **139**, A619–A634 (1965). doi:10.1103/PhysRev.139.A619
[39] P.S. Bagus and H.F. Schaefer, J. Chem. Phys. **55** (3), 1474–1475 (1971). doi:10.1063/1.1676248
[40] P.S. Bagus and H.F. Schaefer, J. Chem. Phys. **56** (1), 224–226 (1972). doi:10.1063/1.1676850
[41] R. Manne and T. Åberg, Chem. Phys. Lett. **7** (2), 282–284 (1970). doi:10.1016/0009-2614(70)80309-8
[42] J.C. Slater and K.H. Johnson, Phys. Rev. B **5**, 844–853 (1972). doi:10.1103/PhysRevB.5.844
[43] J. Ortiz, R. Basu and Y. Öhrn, Chem. Phys. Lett. **103** (1), 29–34 (1983). doi:10.1016/0009-2614(83)87067-5
[44] R. Flores-Moreno, V.G. Zakrzewski and J.V. Ortiz, J. Chem. Phys. **127** (13), 134106 (2007). doi:10.1063/1.2784638
[45] S. Jana and J.M. Herbert, J. Chem. Theory Comput. **19** (13), 4100–4113 (2023). doi:10.1021/acs.jctc.3c00202
[46] S. Jana and J.M. Herbert, J. Chem. Phys. **158** (9), 094111 (2023). doi:10.1063/5.0134459
[47] K. Hirao, T. Nakajima, B. Chan and H.J. Lee, J. Chem. Phys. **158** (6), 064112 (2023). doi:10.1063/5.0140032
[48] G.L.S. Rodrigues, E. Diesen, J. Voss, P. Norman and L.G.M. Pettersson, Struct. Dyn. **9** (1), 014101 (2022). doi:10.1063/4.0000135
[49] L. Triguero, L.G.M. Pettersson and H. Ågren, Phys. Rev. B **58**, 8097–8110 (1998). doi:10.1103/PhysRevB.58.8097
[50] C. Ehlert and T. Klamroth, J. Comput. Chem. **41** (19), 1781–1789 (2020). doi:10.1002/jcc.v41.19
[51] M. Cavalleri, M. Odelius, D. Nordlund, A. Nilsson and L.G.M. Pettersson, Phys. Chem. Chem. Phys.**7**, 2854–2858 (2005). doi:10.1039/b505723j
[52] G.S. Michelitsch and K. Reuter, J. Chem. Phys. **150** (7), 074104 (2019). doi:10.1063/1.5083618
[53] B.P. Klein, S.J. Hall and R.J. Maurer, J. Phys. Condens. Matter **33** (15), 154005 (2021). doi:10.1088/1361-648X/abdf00
[54] N.A. Besley, Acc. Chem. Res. **53** (7), 1306–1315 (2020). doi:10.1021/acs.accounts.0c00171
[55] E.A. Haugen, D. Hait, V. Scutelnic, T. Xue, M. Head-Gordon and S.R. Leone, J. Phys. Chem. A **127** (3), 634–644 (2023). doi:10.1021/acs.jpca.2c06044
[56] E. Ridente, D. Hait, E.A. Haugen, A.D. Ross, D.M. Neumark, M. Head-Gordon and S.R. Leone, Science **380** (6646), 713–717 (2023). doi:10.1126/science.adg4421
[57] N. Pueyo Bellafont, P.S. Bagus, C. Sousa and F. Illas, J. Chem. Phys. **147** (2), 024106 (2017). doi:10.1063/1.4991833
[58] B.G. Janesko, J. Chem. Theory Comput. **19** (3), 837–847 (2023). doi:10.1021/acs.jctc.2c01023
[59] J.M. Kahk, G.S. Michelitsch, R.J. Maurer, K. Reuter and J. Lischner, J. Phys. Chem. Lett. **12** (38), 9353–9359 (2021). doi:10.1021/acs.jpclett.1c02380
[60] W. Park, M. Alías-Rodríguez, D. Cho, S. Lee, M. Huix-Rotllant and C.H. Choi, J. Chem. Theory Comput. **18** (10), 6240–6250 (2022). doi:10.1021/acs.jctc.2c00746
[61] H. Ågren, V. Carravetta, O. Vahtras and L.G. Pettersson, Chem. Phys. Lett. **222** (1), 75–81 (1994).
[62] D. Hait, K.J. Oosterbaan, K. Carter-Fenk and M. Head-Gordon, J. Chem. Phys. **156** (20), 201104 (2022). doi:10.1063/5.0092987
[63] Y. Zhang, J.D. Biggs, D. Healion, N. Govind and S. Mukamel, J. Chem. Phys. **137** (19), 194306 (2012). doi:10.1063/1.4766356

[64] K. Lopata, B.E. Van Kuiken, M. Khalil and N. Govind, J. Chem. Theory Comput. **8** (9), 3284–3292 (2012). doi:10.1021/ct3005613

[65] N.A. Besley, J. Chem. Theory Comput. **12** (10), 5018–5025 (2016). doi:10.1021/acs.jctc.6b00656

[66] J.D. Wadey and N.A. Besley, J. Chem. Theory Comput. **10** (10), 4557–4564 (2014). doi:10.1021/ct500566k

[67] M.W.D. Hanson-Heine, M.W. George and N.A. Besley, J. Chem. Phys. **146** (9), 094106 (2017). doi:10.1063/1.4977178

[68] K. Carter-Fenk, L.A. Cunha, J.E. Arias-Martinez and M. Head-Gordon, J. Phys. Chem. Lett. **13** (41), 9664–9672 (2022). doi:10.1021/acs.jpclett.2c02564

[69] N.A. Besley, M.J.G. Peach and D.J. Tozer, Phys. Chem. Chem. Phys. **11** (44), 10350 (2009). doi:10.1039/b912718f

[70] M.L. Shelby, P.J. Lestrange, N.E. Jackson, K. Haldrup, M.W. Mara, A.B. Stickrath, D. Zhu, H.T. Lemke, M. Chollet, B.M. Hoffman, X. Li and L.X. Chen, J. Am. Chem. Soc. **138** (28), 8752–8764 (2016). doi:10.1021/jacs.6b02176

[71] D. Hait and M. Head-Gordon, J. Phys. Chem. Lett. **11** (3), 775–786 (2020). doi:10.1021/acs.jpclett.9b03661

[72] D. Hait, E.A. Haugen, Z. Yang, K.J. Oosterbaan, S.R. Leone and M. Head-Gordon, J. Chem. Phys.**153** (13), 134108 (2020). doi:10.1063/5.0018833

[73] P. Verma and R.J. Bartlett, J. Chem. Phys. **145** (3), 034108 (2016). doi:10.1063/1.4955194

[74] Y. Jin and R.J. Bartlett, J. Chem. Phys. **149** (6), 064111 (2018). doi:10.1063/1.5038434

[75] Y.C. Park, A. Perera and R.J. Bartlett, J. Chem. Phys. **157** (9), 094107 (2022). doi:10.1063/5.0111095

[76] Y. Yao, D. Golze, P. Rinke, V. Blum and Y. Kanai, J. Chem. Theory Comput. **18** (3), 1569–1583 (2022). doi:10.1021/acs.jctc.1c01180

[77] D. Golze, L. Keller and P. Rinke, J. Phys. Chem. Lett. **11** (5), 1840–1847 (2020). doi:10.1021/acs.jpclett.9b03423

[78] J. Vinson, J.J. Rehr, J.J. Kas and E.L. Shirley, Phys. Rev. B **83**, 115106 (2011). doi:10.1103/PhysRevB.83.115106

[79] J. Vinson and J.J. Rehr, Phys. Rev. B **86**, 195135 (2012). doi:10.1103/PhysRevB.86.195135

[80] D. Golze, M. Dvorak and P. Rinke, Front. Chem. **7**, 377 (2019). doi:10.3389/fchem.2019.00377

[81] K. Gilmore, J. Vinson, E. Shirley, D. Prendergast, C. Pemmaraju, J. Kas, F. Vila and J. Rehr, Comput. Phys. Commun. **197**, 109–117 (2015). doi:10.1016/j.cpc.2015.08.014

[82] R.L. Panadés-Barrueta and D. Golze, J. Chem. Theory Comput. **19**, 5450–5464 (2023). doi:10.1021/acs.jctc.3c00555

[83] T. Zhu and G.K.L. Chan, J. Chem. Theory Comput. **17** (2), 727–741 (2021). doi:10.1021/acs.jctc.0c00704

[84] A. Barth and J. Schirmer, J. Phys. B: At. Mol. Phys. **18** (5), 867 (1985). doi:10.1088/0022-3700/18/5/008

[85] J. Wenzel, M. Wormit and A. Dreuw, J. Chem. Theory Comput. **10** (10), 4583–4598 (2014). doi:10.1021/ct5006888

[86] J. Wenzel, M. Wormit and A. Dreuw, J. Comput. Chem. **35** (26), 1900–1915 (2014). doi:10.1002/jcc.v35.26

[87] C.E.V. de Moura and A.Y. Sokolov, Phys. Chem. Chem. Phys. **24**, 4769–4784 (2022). doi:10.1039/D1CP05476G

[88] T. Fransson and A. Dreuw, J. Chem. Theory Comput. **15** (1), 546–556 (2019). doi:10.1021/acs.jctc.8b01046

[89] J. Wenzel, A. Holzer, M. Wormit and A. Dreuw, J. Chem. Phys. **142** (21), 214104 (2015). doi:10.1063/1.4921841

[90] X. Zheng and L. Cheng, J. Chem. Theory Comput. **15** (9), 4945–4955 (2019). doi:10.1021/acs.jctc.9b00568

[91] X. Zheng, J. Liu, G. Doumy, L. Young and L. Cheng, J. Phys. Chem. A **124** (22), 4413–4426 (2020). doi:10.1021/acs.jpca.0c00901

[92] X. Zheng, C. Zhang, Z. Jin, S.H. Southworth and L. Cheng, Phys. Chem. Chem. Phys. **24** (22), 13587–13596 (2022). doi:10.1039/D2CP00993E

[93] J.E. Arias-Martinez, L.A. Cunha, K.J. Oosterbaan, J. Lee and M. Head-Gordon, Phys. Chem. Chem. Phys. **24** (35), 20728–20741 (2022). doi:10.1039/D2CP01998A

[94] Y.C. Park, A. Perera and R.J. Bartlett, J. Chem. Phys. **151** (16), 164117 (2019). doi:10.1063/1.5117841

[95] Y.C. Park, A. Perera and R.J. Bartlett, J. Chem. Phys. **155** (9), 094103 (2021). doi:10.1063/5.0059276

[96] M. Nooijen and R.J. Bartlett, J. Chem. Phys. **102** (17), 6735–6756 (1995). doi:10.1063/1.469147

[97] M.L. Vidal, X. Feng, E. Epifanovsky, A.I. Krylov and S. Coriani, J. Chem. Theory Comput. **15** (5), 3117–3133 (2019). doi:10.1021/acs.jctc.9b00039

[98] D.R. Nascimento and A.E.I. DePrince, J. Phys. Chem. Lett. **8** (13), 2951–2957 (2017). doi:10.1021/acs.jpclett.7b01206

[99] M. Simons and D.A. Matthews, J. Chem. Theory Comput. **18** (6), 3759–3765 (2022). doi:10.1021/acs.jctc.2c00268

[100] D.A. Matthews, Mol. Phys. **118** (21-22), e1771448 (2020). doi:10.1080/00268976.2020.1771448

[101] C. Liegener and H. Ågren, Theor. Chim. Acta **89** (5-6), 335–362 (1994). doi:10.1007/BF01114106

[102] U. Ekström, P. Norman, V. Carravetta and H. Ågren, Phys. Rev. Lett. **97**, 143001 (2006). doi:10.1103/PhysRevLett.97.143001

[103] A.Y. Zamani and H.P. Hratchian, J. Chem. Phys. **157** (8), 084115 (2022). doi:10.1063/5.0100638

[104] J.M. Kahk and J. Lischner, J. Chem. Theory Comput. **19** (11), 3276–3283 (2023). doi:10.1021/acs.jctc.3c00121

[105] A. Barth, R.J. Buenker, S.D. Peyerimhoff and W. Butscher, Chem. Phys. **46** (1), 149–164 (1980). doi:10.1016/0301-0104(80)85091-9

[106] W. Butscher, R.J. Buenker and S.D. Peyerimhoff, Chem. Phys. Lett. **52** (3), 449–456 (1977). doi:10.1016/0009-2614(77)80484-3

[107] T.N. Rescigno and A.E. Orel, J. Chem. Phys. **70** (7), 3390–3394 (1979). doi:10.1063/1.437870

[108] N. Saito, N. Douguet, H. Sannohe, N. Ishii, T. Kanai, Y. Wu, A. Chew, S. Han, B.I. Schneider, J. Olsen, L. Argenti, Z. Chang and J. Itatani, Phys. Rev. Res. **3**, 043222 (2021). doi:10.1103/PhysRevResearch.3.043222

[109] J.P. Coe and M.J. Paterson, Theor. Chem. Acc. **134** (5), 58 (2015). doi:10.1007/s00214-015-1656-0

[110] S.M. Garner and E. Neuscamman, J. Chem. Phys. **153** (15), 154102 (2020). doi:10.1063/5.0020595

[111] T.S. Hardikar and E. Neuscamman, J. Chem. Phys. **153** (16), 164108 (2020). doi:10.1063/5.0019557

[112] K.J. Oosterbaan, A.F. White and M. Head-Gordon, J. Chem. Phys. **149** (4), 044116 (2018). doi:10.1063/1.5023051
[113] K.J. Oosterbaan, A.F. White and M. Head-Gordon, J. Chem. Theory Comput. **15** (5), 2966–2973 (2019). doi:10.1021/acs.jctc.8b01259
[114] K.J. Oosterbaan, A.F. White, D. Hait and M. Head-Gordon, Phys. Chem. Chem. Phys. **22**, 8182–8192 (2020). doi:10.1039/C9CP06592J
[115] D. Maganas, S. DeBeer and F. Neese, Inorg. Chem. **56** (19), 11819–11836 (2017). doi:10.1021/acs.inorgchem.7b01810
[116] D. Maganas, S. DeBeer and F. Neese, J. Phys. Chem. A **122** (5), 1215–1227 (2018). doi:10.1021/acs.jpca.7b10880
[117] A. Kubas, M. Verkamp, J. Vura-Weis, F. Neese and D. Maganas, J. Chem. Theory Comput. **14** (8), 4320–4334 (2018). doi:10.1021/acs.jctc.8b00302
[118] P.S. Bagus, C. Sousa and F. Illas, J. Chem. Phys. **145** (14), 144303 (2016). doi:10.1063/1.4964320
[119] P.S. Bagus, G. Pacchioni and F. Parmigiani, Chem. Phys. Lett. **207** (4), 569–574 (1993). doi:10.1016/0009-2614(93)89049-N
[120] M. Guo, E. Källman, L.K. Sørensen, M.G. Delcey, R.V. Pinjari and M. Lundberg, J. Phys. Chem. A **120** (29), 5848–5855 (2016). doi:10.1021/acs.jpca.6b05139
[121] P.S. Bagus and B.O. Roos, J. Chem. Phys. **75** (12), 5961–5962 (1981). doi:10.1063/1.442053
[122] M. Alagia, E. Bodo, P. Decleva, S. Falcinelli, A. Ponzi, R. Richter and S. Stranges, Phys. Chem. Chem. Phys. **15**, 1310–1318 (2013). doi:10.1039/C2CP43466K
[123] L.S. Cederbaum, W. Domcke and J. Schirmer, Phys. Rev. A **22**, 206–222 (1980). doi:10.1103/PhysRevA.22.206
[124] S. Ranga and A.K. Dutta, J. Chem. Theory Comput. **17** (12), 7428–7446 (2021). doi:10.1021/acs.jctc.1c00402
[125] J.H. Andersen, K.D. Nanda, A.I. Krylov and S. Coriani, J. Chem. Theory Comput. **18** (10), 6189–6202 (2022). doi:10.1021/acs.jctc.2c00541
[126] M.F. Herbst and T. Fransson, J. Chem. Phys. **153** (5), 054114 (2020). doi:10.1063/5.0013538
[127] P. Pyykkö, in *Advances in Quantum Chemistry*, edited by P.-O. Löwdin (1978), Vol. 11, pp. 353–409.
[128] W. Liu, Mol. Phys. **108** (13), 1679–1706 (2010). doi:10.1080/00268971003781571
[129] W. Liu, J. Chem. Phys. **152** (18), 180901 (2020). doi:10.1063/5.0008432
[130] J.M. Kasper, X. Li, S.A. Kozimor, E.R. Batista and P. Yang, J. Chem. Theory Comput. **18** (4), 2171–2179 (2022). doi:10.1021/acs.jctc.1c00851
[131] A. Grofe and X. Li, Phys. Chem. Chem. Phys. **24** (18), 10745–10756 (2022). doi:10.1039/D2CP01127A
[132] P.S. Bagus, M.J. Sassi and K.M. Rosso, J. Electron. Spectrosc. Relat. Phenom. **200**, 174–180 (2015). doi:10.1016/j.elspec.2015.04.021Special Anniversary Issue: Volume 200.
[133] M. Kehry, Y.J. Franzke, C. Holzer and W. Klopper, Mol. Phys. **118** (21-22), e1755064 (2020). doi:10.1080/00268976.2020.1755064
[134] T. Fransson, D. Burdakova and P. Norman, Phys. Chem. Chem. Phys. **18**, 13591–13603 (2016). doi:10.1039/C6CP00561F
[135] L. Konecny, J. Vicha, S. Komorovsky, K. Ruud and M. Repisky, Inorg. Chem. **61** (2), 830–846 (2022). doi:10.1021/acs.inorgchem.1c02412
[136] U. Ekström, P. Norman and V. Carravetta, Phys. Rev. A **73**, 022501 (2006). doi:10.1103/PhysRevA.73.022501
[137] T. Zhang, J.M. Kasper and X. Li, in *Annual Reports in Computational Chemistry*, edited by D.A. Dixon (2020), Vol. 16, pp. 17–37.
[138] B. Pickup and O. Goscinski, Mol. Phys. **26** (4), 1013–1035 (1973). doi:10.1080/00268977300102261
[139] Y. Imamura and H. Nakai, Int. J. Quantum Chem. **107** (1), 23–29 (2007). doi:10.1002/qua.v107:1
[140] W. Schwarz, T. Chang, U. Seeger and K. Hwang, Chem. Phys. **117** (1), 73–89 (1987). doi:10.1016/0301-0104(87)80098-8
[141] L.S. Cederbaum, F. Tarantelli, A. Sgamellotti and J. Schirmer, J. Chem. Phys. **85** (11), 6513–6523 (1986). doi:10.1063/1.451432
[142] L.C. Snyder, J. Chem. Phys. **55** (1), 95–99 (1971). doi:10.1063/1.1675565
[143] L. Hedin and A. Johansson, J. Phys. B: Atom. Mol. Phys. **2** (12), 1336–1346 (1969). doi:10.1088/0022-3700/2/12/313
[144] J.A.D. Matthew and R.S. Perkins, J. Phys. C: Solid State Phys. **11** (14), L569–L574 (1978). doi:10.1088/0022-3719/11/14/002
[145] L.S. Cederbaum and W. Domcke, J. Chem. Phys. **66** (11), 5084–5086 (1977). doi:10.1063/1.433763
[146] A. Szabo and N.S. Ostlund, *Modern Quantum Chemistry* Dover Books on Chemistry (Dover Publications, Mineola, NY, 1996).
[147] G. Born, H.A. Kurtz and Y. Öhrn, J. Chem. Phys. **68** (1), 74–85 (1978). doi:10.1063/1.435475
[148] B. Wästberg, S. Lunell, C. Enkvist, P.A. Brühwiler, A.J. Maxwell and N. Mårtensson, Phys. Rev. B **50**, 13031–13034 (1994). doi:10.1103/PhysRevB.50.13031
[149] D.J. Thouless, *The Quantum Mechanics of Many-Body Systems: Second Edition* (Dover Publications, Mineola, NY, 1990).
[150] D. Hait and M. Head-Gordon, J. Phys. Chem. Lett. **12** (19), 4517–4529 (2021). doi:10.1021/acs.jpclett.1c00744
[151] T.J. Watson and R.J. Bartlett, Chem. Phys. Lett. **555**, 235–238 (2013). doi:10.1016/j.cplett.2012.08.046
[152] A.Y. Zamani, Ph. D. thesis, University of California, Merced, 2023.
[153] S. Dasgupta, C. Shahi, P. Bhetwal, J.P. Perdew and F. Paesani, J. Chem. Theory Comput. **18** (8), 4745–4761 (2022). doi:10.1021/acs.jctc.2c00313
[154] K.R. Bryenton, A.A. Adeleke, S.G. Dale and E.R. Johnson, Wiley Interdiscip. Rev.: Comput. Mol. Sci. **13** (2), e1631 (2023).
[155] M.C. Kim, E. Sim and K. Burke, Phys. Rev. Lett. **111**, 073003 (2013). doi:10.1103/PhysRevLett.111.073003
[156] M.C. Kim, E. Sim and K. Burke, J. Chem. Phys. **140** (18), 18A528 (2014). doi:10.1063/1.4869189
[157] S. Vuckovic, S. Song, J. Kozlowski, E. Sim and K. Burke, J. Chem. Theory Comput. **15** (12), 6636–6646 (2019). doi:10.1021/acs.jctc.9b00826
[158] R.J. Bartlett and Y. Öhrn, Theor. Chim. Acta **21** (3), 215–234 (1971). doi:10.1007/BF01172014

[159] A.T.B. Gilbert, N.A. Besley and P.M.W. Gill, J. Phys. Chem. A **112** (50), 13164–13171 (2008). doi:10.1021/jp801738f

[160] N.A. Besley, A.T.B. Gilbert and P.M.W. Gill, J. Chem. Phys. **130** (12), 124308 (2009). doi:10.1063/1.3092928

[161] H.H. Corzo, A. Abou Taka, A. Pribram-Jones and H.P. Hratchian, J. Comput. Chem. **43** (6), 382–390 (2022). doi:10.1002/jcc.v43.6

[162] A. Abou Taka, S.Y. Lu, D. Gowland, T.J. Zuehlsdorff, H.H. Corzo, A. Pribram-Jones, L. Shi, H.P. Hratchian and C.M. Isborn, J. Chem. Theory Comput. **18** (5), 3039–3051 (2022). doi:10.1021/acs.jctc.1c01127

[163] A. Abou Taka, H.H. Corzo, A. Pribram-Jones and H.P. Hratchian, J. Chem. Theory Comput. **18** (12), 7286–7297 (2022). doi:10.1021/acs.jctc.2c00672

[164] G. Macetti and A. Genoni, Molecules **28** (1), 136 (2023). doi:10.3390/molecules28010136

[165] K. Carter-Fenk and J.M. Herbert, J. Chem. Theory Comput. **16** (8), 5067–5082 (2020). doi:10.1021/acs.jctc.0c00502

[166] D. Hait and M. Head-Gordon, J. Chem. Theory Comput. **16** (3), 1699–1710 (2020). doi:10.1021/acs.jctc.9b01127

[167] P. Lykos and G.W. Pratt, Rev. Mod. Phys. **35**, 496–501 (1963). doi:10.1103/RevModPhys.35.496

[168] H. Fukutome, Prog. Theor. Phys. **45** (5), 1382–1406 (1971). doi:10.1143/PTP.45.1382

[169] H. Fukutome, Prog. Theor. Phys. **52** (1), 115–130 (1974). doi:10.1143/PTP.52.115

[170] H. Fukutome, Prog. Theor. Phys. **52** (6), 1766–1783 (1974). doi:10.1143/PTP.52.1766

[171] L. Noodleman, J. Chem. Phys. **74** (10), 5737–5743 (1981). doi:10.1063/1.440939

[172] K. Yamaguchi, F. Jensen, A. Dorigo and K. Houk, Chem. Phys. Lett. **149** (5), 537–542 (1988). doi:10.1016/0009-2614(88)80378-6

[173] L.M. Thompson and H.P. Hratchian, Mol. Phys. **117** (9-12), 1421–1429 (2019). doi:10.1080/00268976.2018.1554828

[174] B.N. Plakhutin, E.V. Gorelik, N.N. Breslavskaya, M.A. Milov, A. Fokeyev, A.V. Novikov, T.E. Prokhorov, N.E. Polygalova, S.P. Dolin and L.I. Trakhtenberg, J. Struct. Chem. **46** (2), 195–203 (2005). doi:10.1007/s10947-006-0031-3

[175] N. Koga, K. Yamashita and K. Morokuma, Chem. Phys. Lett. **184** (4), 359–362 (1991). doi:10.1016/0009-2614(91)85137-L

[176] N.M. Gray and L.A. Wills, Phys. Rev. **38**, 248–254 (1931). doi:10.1103/PhysRev.38.248

[177] G.W. Pratt, Phys. Rev. **92**, 278–288 (1953). doi:10.1103/PhysRev.92.278

[178] P.O. Löwdin, Phys. Rev. **97**, 1509–1520 (1955). doi:10.1103/PhysRev.97.1509

[179] A. Rotenberg, J. Chem. Phys. **39** (3), 512–517 (1963). doi:10.1063/1.1734286

[180] R. Pauncz, *Spin Eigenfunctions: Construction and Use* (Springer, New York, NY, 1979).

[181] I. Shavitt, in *The Unitary Group for the Evaluation of Electronic Energy Matrix Elements*, edited by J. Hinze (Springer Berlin Heidelberg, Berlin, Heidelberg, 1981), pp. 51–99.

[182] W.A. Goddard, Phys. Rev. **157**, 73–80 (1967). doi:10.1103/PhysRev.157.73

[183] C.R. Sarma, M.A.H. Ahsan and S. Rettrup, Int. J. Quantum Chem. **58** (6), 637–643 (1996). doi:10.1002/(ISSN)1097-461X

[184] W.I. Salmon, in *Advances in Quantum Chemistry*, edited by P.-O. Lowdin (1974), Vol. 8, pp. 37–94.

[185] P.O. Löwdin, Rev. Mod. Phys. **36**, 966–976 (1964). doi:10.1103/RevModPhys.36.966

[186] T. Amos and L.C. Snyder, J. Chem. Phys. **41** (6), 1773–1783 (1964). doi:10.1063/1.1726157

[187] P.O. Löwdin, Phys. Rev. **97**, 1474–1489 (1955). doi:10.1103/PhysRev.97.1474

[188] P.O. Löwdin and O. Goscinski, Int. J. Quantum Chem. **4** (S3B), 533–591 (1969). doi:10.1002/qua.v4:3b+

[189] J. Smith, H. Vedene and F.E. Harris, J. Math. Phys. **10** (4), 771–778 (1969). doi:10.1063/1.1664904

[190] C.A. Jiménez-Hoyos, T.M. Henderson, T. Tsuchimochi and G.E. Scuseria, J. Chem. Phys. **136** (16), 164109 (2012). doi:10.1063/1.4705280

[191] U. Kaldor, J. Chem. Phys. **48** (2), 835–837 (1968). doi:10.1063/1.1668721

[192] I. Mayer, in *Advances in Quantum Chemistry*, edited by P.-O. Löwdin (1980), Vol. 12, pp. 189–262.

[193] C.F. Bunge, Phys. Rev. **154**, 70–79 (1967). doi:10.1103/PhysRev.154.70

[194] N. Bessis, H. Lefebvre-Brion and C.M. Moser, Phys. Rev. **130**, 1441–1443 (1963). doi:10.1103/PhysRev.130.1441

[195] A.T. Amos, G.G. Hall and H. Jones, Proc. R. Soc. London, Ser. A **263** (1315), 483–493 (1961). doi:10.1098/rspa.1961.0175

[196] P.O. Löwdin, Rev. Mod. Phys. **32**, 328–334 (1960). doi:10.1103/RevModPhys.32.328

[197] C. Møller and M.S. Plesset, Phys. Rev. **46**, 618–622 (1934). doi:10.1103/PhysRev.46.618

[198] I. Ljubić, J. Chem. Theory Comput. **10** (6), 2333–2343 (2014). doi:10.1021/ct500111n

[199] J. Shim, M. Klobukowski, M. Barysz and J. Leszczynski, Phys. Chem. Chem. Phys. **13**, 5703–5711 (2011). doi:10.1039/c0cp01591a

[200] I.E. Brumboiu and T. Fransson, J. Chem. Phys. **156** (21), 214109 (2022). doi:10.1063/5.0088195

[201] N. Kosugi, Chem. Phys. **289** (1), 117–134 (2003). doi:10.1016/S0301-0104(02)00791-7Decay Processes in Core-excited Species.

[202] N.C. Handy, P.J. Knowles and K. Somasundram, Theor. Chim. Acta **68** (1), 87–100 (1985). doi:10.1007/BF00698753

[203] D. Cremer, Wiley Interdiscip. Rev.: Comput. Mol. Sci. **1** (4), 509–530 (2011).

[204] U. Bozkaya and C.D. Sherrill, J. Chem. Phys. **141** (20), 204105 (2014). doi:10.1063/1.4902226

[205] M. Loipersberger, L.W. Bertels, J. Lee and M. Head-Gordon, J. Chem. Theory Comput. **17** (9), 5582–5599 (2021). doi:10.1021/acs.jctc.1c00469

[206] S. Suliman, M. Pitoňák, I. Cernusak and F. Louis, Comput. Theor. Chem. **1186**, 112901 (2020). doi:10.1016/j.comptc.2020.112901

[207] U. Bozkaya, J. Chem. Theory Comput. **10** (5), 2041–2048 (2014). doi:10.1021/ct500186j

[208] H.B. Schlegel, J. Phys. Chem. **92** (11), 3075–3078 (1988). doi:10.1021/j100322a014
[209] P.O. Löwdin, J. Math. Phys. **3** (5), 969–982 (1962). doi:10.1063/1.1724312
[210] W. Chen and H.B. Schlegel, J. Chem. Phys. **101** (7), 5957–5968 (1994). doi:10.1063/1.467312
[211] J. Wang, A.D. Becke, J. Smith and H. Vedene, J. Chem. Phys. **102** (8), 3477–3480 (1995). doi:10.1063/1.468585
[212] H.B. Schlegel, in edited by P. von Ragué Schleyer, N.L. Allinger, T. Clark, J. Gasteiger, P.A. Kollman, H.F. Schaefer and P.R. Schreiner (1998), Chap. Spin Contamination, pp. 2665–2671.
[213] H.B. Schlegel, J. Chem. Phys. **84** (8), 4530–4534 (1986). doi:10.1063/1.450026
[214] R. Krishnan and J.A. Pople, Int. J. Quantum Chem. **14** (1), 91–100 (1978). doi:10.1002/qua.v14:1
[215] H.A. Bethe and E.E. Salpeter, *Quantum Mechanics of One- and Two-Electron Atoms* (Springer Berlin Heidelberg, Berlin Heidelberg, 1957).
[216] C.L. Pekeris, Phys. Rev. **112**, 1649–1658 (1958). doi:10.1103/PhysRev.112.1649
[217] C.W. Scherr and J.N. Silverman, J. Chem. Phys. **37** (5), 1154–1156 (1962). doi:10.1063/1.1733236
[218] D.P. Chong, J. Chem. Phys. **103** (5), 1842–1845 (1995). doi:10.1063/1.469758
[219] G. Cavigliasso and D.P. Chong, J. Chem. Phys. **111** (21), 9485–9492 (1999). doi:10.1063/1.480279
[220] D.P. Chong, J. Electron. Spectrosc. Relat. Phenom. **159** (1), 94–96 (2007). doi:10.1016/j.elspec.2007.01.005
[221] A. Dreuw and T. Fransson, Phys. Chem. Chem. Phys. **24**, 11259–11267 (2022). doi:10.1039/D2CP00584K
[222] B.P. Pritchard, D. Altarawy, B. Didier, T.D. Gibson and T.L. Windus, J. Chem. Inf. Model. **59** (11), 4814–4820 (2019). doi:10.1021/acs.jcim.9b00725
[223] A. Hitchcock and C. Brion, J. Electron. Spectrosc. Relat. Phenom. **10** (3), 317–330 (1977). doi:10.1016/0368-2048(77)85029-9
[224] G.C. King, F.H. Read and M. Tronc, Chem. Phys. Lett. **52** (1), 50–54 (1977). doi:10.1016/0009-2614(77)85118-X
[225] T. Gejo, K. Okada and T. Ibuki, Chem. Phys. Lett. **277** (5), 497–501 (1997). doi:10.1016/S0009-2614(97)00965-2
[226] A.P. Hitchcock and C.E. Brion, J. Phys. B: At. Mol. Phys. **14** (22), 4399 (1981). doi:10.1088/0022-3700/14/22/022
[227] P. Parent, F. Bournel, J. Lasne, S. Lacombe, G. Strazzulla, S. Gardonio, S. Lizzit, J.P. Kappler, L. Joly, C. Laffon and S. Carniato, J. Chem. Phys. **131** (15), 154308 (2009). doi:10.1063/1.3243849
[228] E. Rühl and A. Hitchcock, Chem. Phys. **154** (2), 323–329 (1991). doi:10.1016/0301-0104(91)80082-S
[229] R. McLaren, S.A.C. Clark, I. Ishii and A.P. Hitchcock, Phys. Rev. A **36**, 1683–1701 (1987). doi:10.1103/PhysRevA.36.1683
[230] A. Hitchcock and C. Brion, Chem. Phys. **37** (3), 319–331 (1979). doi:10.1016/0301-0104(79)85032-6
[231] G. Wight and C. Brion, J. Electron. Spectrosc. Relat. Phenom. **3** (3), 191–205 (1974). doi:10.1016/0368-2048(74)80010-1
[232] M. Robin, I. Ishii, R. McLaren and A. Hitchcock, J. Electron. Spectrosc. Relat. Phenom. **47**, 53–92 (1988). doi:10.1016/0368-2048(88)85005-9
[233] P. Cabral do Couto, D. Hollas and P. Slavíček, J. Chem. Theory Comput. **11** (7), 3234–3244 (2015). doi:10.1021/acs.jctc.5b00066
[234] G. Wight and C. Brion, J. Electron. Spectrosc. Relat. Phenom. **4** (4), 313–325 (1974). doi:10.1016/0368-2048(74)80062-9
[235] A.P. Hitchcock, D.C. Newbury, I. Ishii, J. Stöhr, J.A. Horsley, R.D. Redwing, A.L. Johnson and F. Sette, J. Chem. Phys. **85** (9), 4849–4862 (1986). doi:10.1063/1.451719
[236] M.F. Tesch, R. Golnak, F. Ehrhard, D. Schön, J. Xiao, K. Atak, A. Bande and E.F. Aziz, Chem. Eur. J. **22** (34), 12040–12049 (2016). doi:10.1002/chem.v22.34
[237] I. Ishii, R. McLaren, A.P. Hitchcock and M.B. Robin, J. Chem. Phys. **87** (8), 4344–4360 (1987). doi:10.1063/1.452893
[238] D. Duflot, J.P. Flament, A. Giuliani, J. Heinesch and M.J. Hubin-Franskin, J. Chem. Phys. **119** (17), 8946–8955 (2003). doi:10.1063/1.1606441
[239] M. Simon, M. Lavollee, P. Morin and I. Nenner, J. Phys. Chem. **99** (6), 1733–1740 (1995). doi:10.1021/j100006a015
[240] C. Hannay, D. Duflot, J.P. Flament and M.J. Hubin-Franskin, J. Chem. Phys. **110** (12), 5600–5610 (1999). doi:10.1063/1.478458
[241] F. Sette, J. Stöhr and A.P. Hitchcock, J. Chem. Phys. **81** (11), 4906–4914 (1984). doi:10.1063/1.447528
[242] R.N. Sodhi and C. Brion, J. Electron. Spectrosc. Relat. Phenom. **37** (1), 1–21 (1985). doi:10.1016/0368-2048(85)80079-7
[243] S. Michelin, K. Mazon, F. Arretche, W. Tenfen, H. Oliveira, A. Falck, M. Scopel, L. da Silva, M. Fujimoto, I. Iga and M.T. Lee, J. Electron. Spectrosc. Relat. Phenom. **171** (1), 30–36 (2009). doi:10.1016/j.elspec.2009.01.001
[244] I.H. Suzuki and N. Saito, Int. J. Mass Spectrom. **198** (3), 165–172 (2000). doi:10.1016/S1387-3806(00)00186-X
[245] J.A. Horsley, J. Stöhr, A.P. Hitchcock, D.C. Newbury, A.L. Johnson and F. Sette, J. Chem. Phys. **83** (12), 6099–6107 (1985). doi:10.1063/1.449601
[246] D.C. Newbury, I. Ishii and A.P. Hitchcock, Can. J. Chem. **64** (6), 1145–1155 (1986). doi:10.1139/v86-900
[247] D.P. Chong, O.V. Gritsenko and E.J. Baerends, J. Chem. Phys. **116** (5), 1760–1772 (2002). doi:10.1063/1.1430255
[248] R.D. Johnson III, NIST Computational Chemistry Comparison and Benchmark. Database NIST Standard Reference Database Number 101. Release 21. 2020. https://cccbdb.nist.gov/ (Accessed May 5, 2022).
[249] D.S. Ranasinghe, J.T. Margraf, A. Perera and R.J. Bartlett, J. Chem. Phys. **150** (7), 074108 (2019). doi:10.1063/1.5084728
[250] M.J. Frisch, G.W. Trucks, H.B. Schlegel, G.E. Scuseria, M.A. Robb, J.R. Cheeseman, V.B.G. Scalmani, G.A. Petersson, H. Nakatsuji, X. Li, A.V. Marenich, M. Caricato, J. Bloino, B.G. Janesko, J. Zheng, R. Gomperts, B. Mennucci, H.P. Hratchian, J.V. Ortiz, A.F. Izmaylov, J.L. Sonnenberg, D. Williams-Young, F. Ding, F. Lipparini, F. Egidi, J. Goings, B. Peng, A. Petrone, T. Henderson, D. Ranasinghe, V.G. Zakrzewski, J. Gao, N. Rega, G. Zheng, W. Liang, M. Hada, M. Ehara, K. Toyota, R. Fukuda, J. Hasegawa, M. Ishida, T. Nakajima, Y. Honda, O. Kitao, H. Nakai, T. Vreven, K. Throssell, J.A. Montgomery Jr.,

J.E. Peralta, F. Ogliaro, M.J. Bearpark, J.J. Heyd, E.N. Brothers, K.N. Kudin, V.N. Staroverov, T.A. Keith, R. Kobayashi, J. Normand, K. Raghavachari, A.P. Rendell, J.C. Burant, S.S. Iyengar, J. Tomasi, M. Cossi, J.M. Millam, M. Klene, C. Adamo, R. Cammi, J.W. Ochterski, R.L. Martin, K. Morokuma, O. Farkas, J.B. Foresman and D.J. Fox, *Gaussian Development Version, Revision J.15* (Gaussian Inc., Wallingford, CT, 2022).

[251] C.T. Chen, Y. Ma and F. Sette, Phys. Rev. A **40**, 6737–6740 (1989). doi:10.1103/PhysRevA.40.6737

[252] G. Wight, C. Brion and M. Van Der Wiel, J. Electron. Spectrosc. Relat. Phenom. **1** (5), 457–469 (1972). doi:10.1016/0368-2048(72)80016-1

[253] M. Nakamura, M. Sasanuma, S. Sato, M. Watanabe, H. Yamashita, Y. Iguchi, A. Ejiri, S. Nakai, S. Yamaguchi, T. Sagawa, Y. Nakai and T. Oshio, Phys. Rev. **178**, 80–82 (1969). doi:10.1103/PhysRev.178.80

[254] R.H. Myhre, T.J.A. Wolf, L. Cheng, S. Nandi, S. Coriani, M. Gühr and H. Koch, J. Chem. Phys.**148** (6), 064106 (2018). doi:10.1063/1.5011148

[255] J.P. Carbone, L. Cheng, R.H. Myhre, D. Matthews, H. Koch and S. Coriani, in *State of The Art of Molecular Electronic Structure Computations: Correlation Methods, Basis Sets and More*, edited by L. Ugo Ancarani and P.E. Hoggan, *Advances in Quantum Chemistry* (2019), Vol. 79, pp. 241–261.

[256] R. Sarangi, M.L. Vidal, S. Coriani and A.I. Krylov, Mol. Phys. **118** (19-20), e1769872 (2020). doi:10.1080/00268976.2020.1769872

[257] M.A. Ambroise and F. Jensen, J. Chem. Theory Comput. **15** (1), 325–337 (2019). doi:10.1021/acs.jctc.8b01071

[258] D. Hait and T.J. Martínez, J. Chem. Theory Comput. **20** (2), 873–881 (2024). doi:10.1021/acs.jctc.3c01035

[259] J. Adachi, N. Kosugi, E. Shigemasa and A. Yagishita, J. Chem. Phys. **107** (13), 4919–4926 (1997). doi:10.1063/1.474855

[260] E. Muchova, D. Hollas, D.M.P. Holland, C. Bacellar, L. Leroy, T.R. Barillot, L. Longetti, M. Coreno, M. de Simone, C. Grazioli, M. Chergui and R.A. Ingle, Phys. Chem. Chem. Phys. **25**, 6733–6745 (2023). doi:10.1039/D2CP05299G

[261] T. Tsuchimochi and T. Van Voorhis, J. Chem. Phys. **141** (16), 164117 (2014). doi:10.1063/1.4898804

[262] T. Tsuchimochi and S.L. Ten-no, J. Chem. Theory Comput. **15** (12), 6688–6702 (2019). doi:10.1021/acs.jctc.9b00897

[263] A. Annaberdiyev, C.A. Melton, M.C. Bennett, G. Wang and L. Mitas, J. Chem. Theory Comput. **16** (3), 1482–1502 (2020). doi:10.1021/acs.jctc.9b00962

[264] C. Edmiston and K. Ruedenberg, Rev. Mod. Phys. **35**, 457–464 (1963). doi:10.1103/RevModPhys.35.457

[265] S.F. Boys, Rev. Mod. Phys. **32**, 296–299 (1960). doi:10.1103/RevModPhys.32.296

[266] A.A. Jarzęcki and E.R. Davidson, J. Phys. Chem. A **102** (24), 4742–4746 (1998). doi:10.1021/jp981290x

[267] D.G. Oprea and H.G. Burton, in *Advances in Quantum Chemistry*, edited by P.E. Hoggan (2023), Vol. 88, pp. 249–271.

[268] F. Weigend, M. Häser, H. Patzelt and R. Ahlrichs, Chem. Phys. Lett. **294** (1), 143–152 (1998). doi:10.1016/S0009-2614(98)00862-8

[269] U. Bozkaya, J. Chem. Theory Comput. **12** (3), 1179–1188 (2016). doi:10.1021/acs.jctc.5b01128

[270] W. Skomorowski and A.I. Krylov, J. Chem. Phys. **154** (8), 084124 (2021). doi:10.1063/5.0036976

[271] J.V. Ortiz, J. Chem. Phys. **81** (12), 5873–5888 (1984). doi:10.1063/1.447588